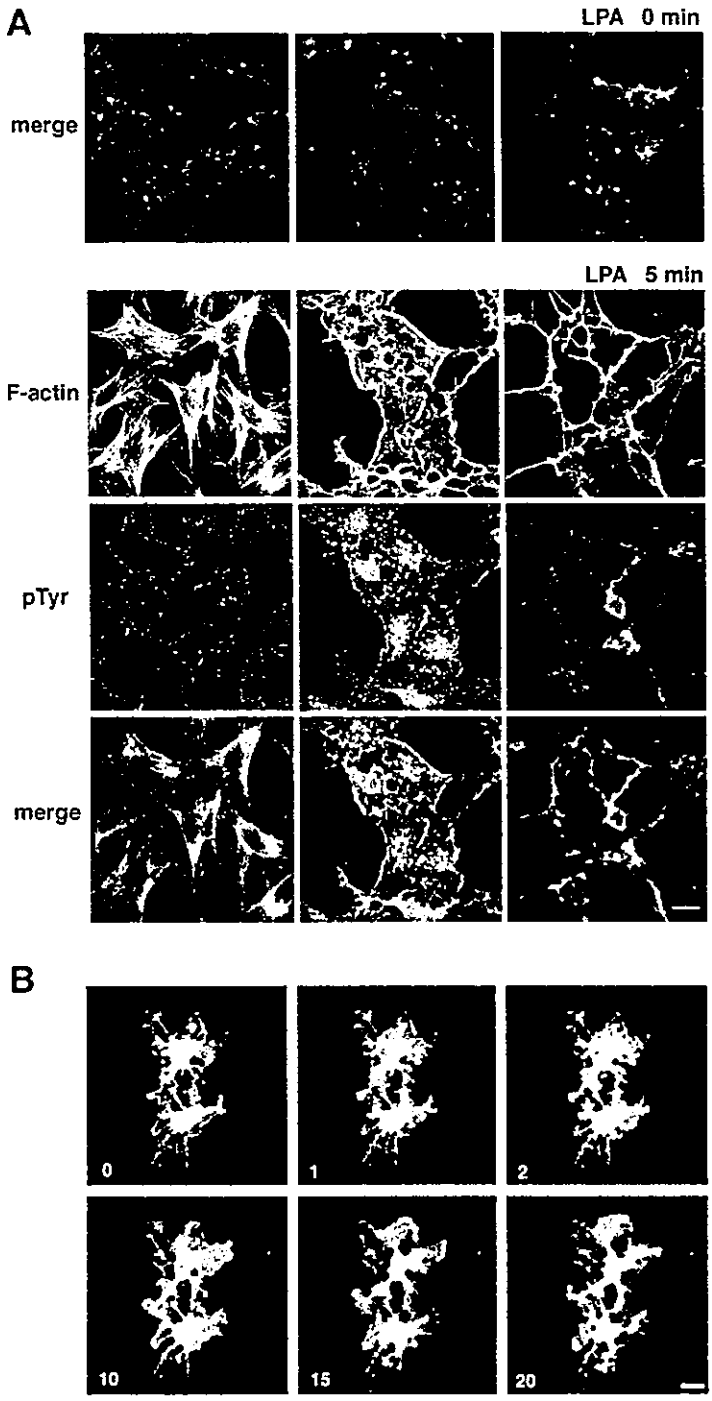

Figure 1. **Effects of C3 exoenzyme and Y-27632 on actin reorganization and localization of tyrosine-phosphorylated proteins in LPA-stimulated Swiss 3T3 cells.** (A) Immunofluorescence. Swiss 3T3 cells were maintained in DME containing 10% FBS for 3 d and cultured in serum-free DME for 24 h. During this period, the cells were without any treatment or treated with either 30 μg/ml C3 exoenzyme for 4 d or with 30 μM Y-27632 for 30 min and then exposed to 5 μM LPA for 0 and 5 min. The cells were fixed, permeabilized, and stained with Texas red phalloidin for F-actin (red) and antiphosphotyrosine antibody (green). The top panels show the merged images of the cells without LPA stimulation. The F-actin staining, the phosphotyrosine staining, and the merged images of the LPA-stimulated cells are shown in the second, third, and the bottom rows of the panels, respectively. Note that the cells treated with Y-27632 display a thick rim of F-actin and dot-like phosphotyrosine staining in the cell periphery upon the addition of LPA. (B) Video microscopy. Swiss 3T3 cells transfected with GFP actin were serum starved for 24 h and treated with 30 μM Y-27632 for the last 30 min. LPA was added at 5 μM, and the cell shape change was monitored in the continued presence of Y-27632 by time-lapse confocal microscopy as the image of GFP actin. The number in each image indicates time after the LPA addition in min. See also the video available at http://www.jcb.org/cgi/content/full/jcb.200112107/DC1. Bars, 20 μm.

Tyrosine phosphorylation of p130Cas occurs through the Rho-dependent, ROCK-independent signaling

To elucidate the above Rho-dependent, ROCK-independent signaling biochemically, we compared the effects of C3 exoenzyme and Y-27632 on LPA-induced tyrosine phosphorylation of focal adhesion proteins. Swiss 3T3 cells were treated with either vehicle, C3 exoenzyme, or Y-27632 for the indicated times and then stimulated with LPA for 0, 5, and 30 min. Cell lysates were prepared and subjected to immunoblotting and immunoprecipitation analysis. As shown in Fig. 3 A, LPA addition induced tyrosine phosphorylation of proteins of ~70 and 120–130 kD, which correspond to a group of phosphorylated paxillin isoforms and a combined band of p125FAK and p130Cas, respectively. The C3 exoenzyme treatment suppressed tyrosine phosphorylation of both groups of proteins as reported previously (Kumagai et

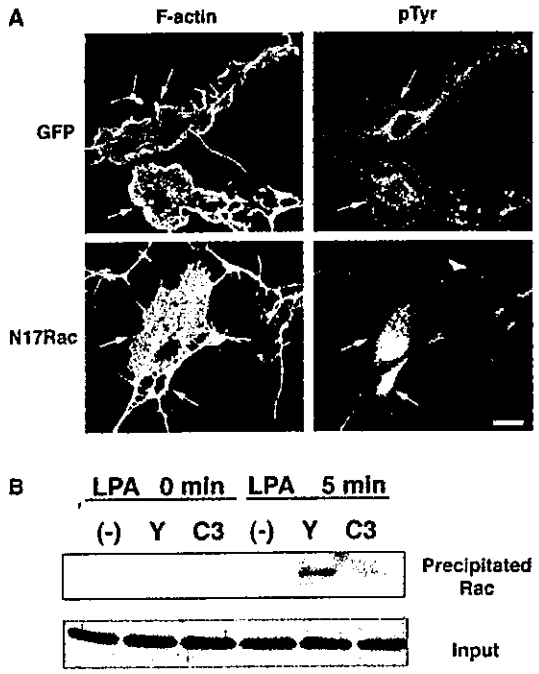

Figure 2. **LPA-induced Rac activation in Y-27632–treated Swiss 3T3 cells.** (A) Inhibition of membrane ruffles by expression of N17Rac in Y-27632–treated cells. Swiss 3T3 cells were transfected with 1 μg of pCMV5–N17Rac or 1 μg of pEGFP–C1. The transfected cells were cultured in DME containing 10% FBS for 16 h and then in serum-free DME for 24 h. The cells were treated with 30 μM Y-27632 for 30 min and then stimulated with LPA for 5 min. The cells were stained for F-actin and phosphotyrosine as described in the legend to Fig. 1. Arrows indicate transfected cells identified with anti-GFP (top) or anti-Flag staining (bottom). Note that membrane ruffles and focal complexes disappeared in the cells overexpressing N17Rac. Bar, 20 μm. (B) Pull-down assay for GTP-Rac. Swiss 3T3 cells were cultured and treated with either C3 exoenzyme or Y-27632 as described in the legend to Fig. 1. The cells were then stimulated with 5 μM LPA for 0 and 5 min and subjected to the pull-down assay as described in Materials and methods. GTP-Rac precipitated from each cell lysates was analyzed by immunoblotting with anti-Rac antibody (top), and the total amounts of Rac present in the cell lysates are shown in the immunoblot in the bottom panels. −, cells without any pretreatment; Y, cells treated with Y-27632; C3, cells treated with C3 exoenzyme. Note that GTP-Rac increased in amount significantly by Y-27632 treatment and remained little in the C3 exoenzyme-treated cells.

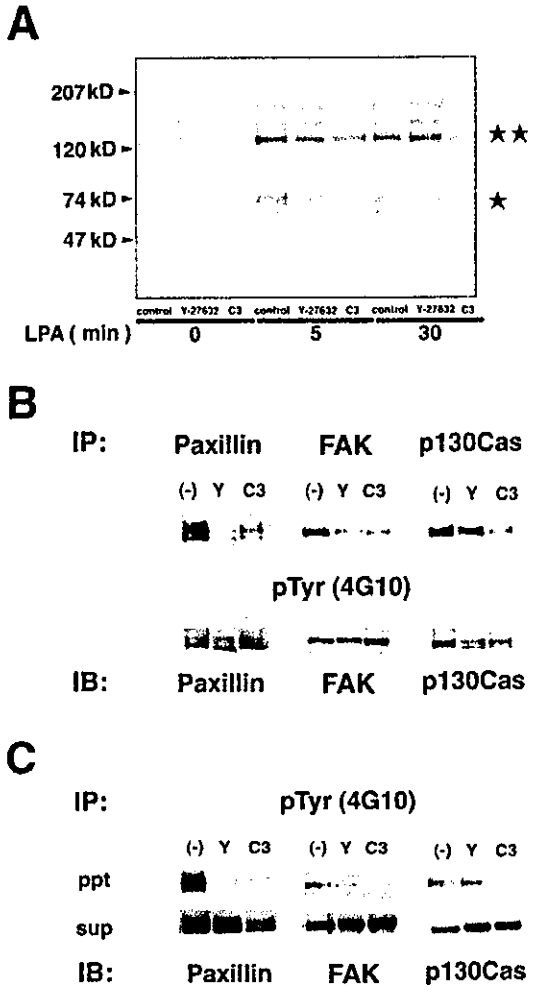

Figure 3. **Different effects of C3 exoenzyme and Y-27632 on tyrosine phosphorylation of focal adhesion proteins.** (A) Effects of C3 exoenzyme and Y-27632 on LPA-induced tyrosine phosphorylation. Swiss 3T3 cells were cultured and treated either with none, C3 exoenzyme, or Y-27632 as described in the legend to Fig. 1. The cells were then stimulated with 5 μM LPA for 0, 5, and 30 min. The cell lysates were prepared and subjected to SDS-PAGE and immunoblotting using antiphosphotyrosine antibody. A single asterisk and double asterisk indicate the tyrosine-phosphorylated paxillin isoforms and the combined band of phosphorylated FAK and Cas, respectively. (B and C) Inhibition of tyrosine phosphorylation of FAK and paxillin but not that of Cas by Y-27632 treatment. The lysates of cells stimulated with LPA for 5 min were subjected to immunoprecipitation using either antipaxillin, anti-FAK, or anti-p130Cas antibodies (B) or using antiphosphotyrosine antibody (C). The immunoprecipitates were then analyzed by immunoblotting with antiphosphotyrosine antibody (B) or with antipaxillin, anti-FAK, and anti-p130Cas antibodies (C). −, cells without any pretreatment; Y, cells treated with Y-27632; C3, cells treated with C3 exoenzyme. Note that Y-27632 treatment suppressed tyrosine phosphorylation of paxillin and FAK but not that of Cas, whereas the phosphorylation of these three proteins were equally suppressed by C3 exoenzyme treatment.

al., 1993; Rankin et al., 1994; Needham and Rozengurt, 1998). On the other hand, Y-27632 suppressed tyrosine phosphorylation of the 70-kD group but only partially affected that of the 120–130-kD group. The tyrosine phosphorylation of the latter group declined at 30 min in the control cells, whereas it remained high in the Y-27632–treated cells. Immunoprecipitation experiments using antipaxillin, anti-FAK, and anti-Cas antibodies revealed that Y-27632 treatment suppressed tyrosine phosphorylation of paxillin and FAK to the extent similar to that achieved by C3 exoenzyme treatment, whereas it barely inhibited the phosphorylation of Cas (Fig. 3 B). The same result was obtained by immunoblotting with antipaxillin, anti-FAK, and anti-Cas antibodies of proteins precipitated with antiphosphotyrosine monoclonal antibody (Fig. 3 C). These results suggest the presence of a dichotomy of the signaling from Rho to the tyrosine phosphorylation of focal adhesion pro-

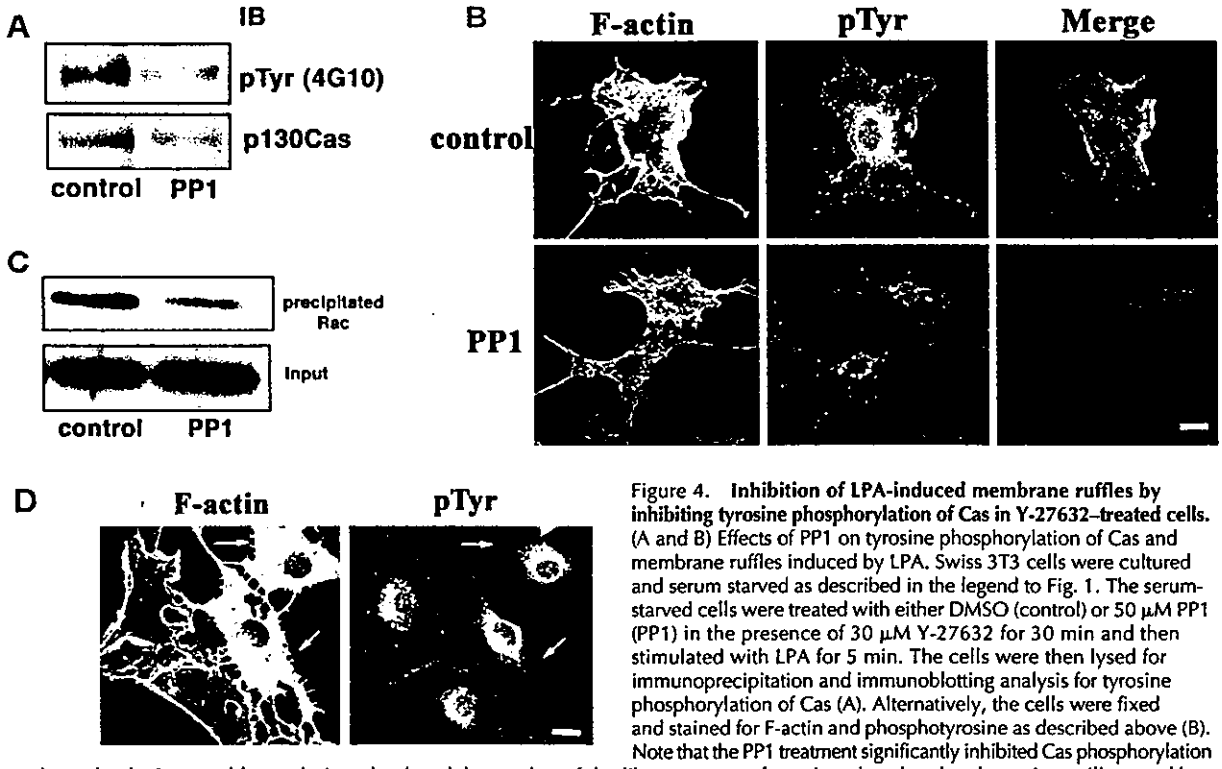

Figure 4. **Inhibition of LPA-induced membrane ruffles by inhibiting tyrosine phosphorylation of Cas in Y-27632–treated cells.** (A and B) Effects of PP1 on tyrosine phosphorylation of Cas and membrane ruffles induced by LPA. Swiss 3T3 cells were cultured and serum starved as described in the legend to Fig. 1. The serum-starved cells were treated with either DMSO (control) or 50 μM PP1 (PP1) in the presence of 30 μM Y-27632 for 30 min and then stimulated with LPA for 5 min. The cells were then lysed for immunoprecipitation and immunoblotting analysis for tyrosine phosphorylation of Cas (A). Alternatively, the cells were fixed and stained for F-actin and phosphotyrosine as described above (B). Note that the PP1 treatment significantly inhibited Cas phosphorylation as shown by the immunoblot analysis and reduced the number of dot-like structures of tyrosine-phosphorylated proteins as illustrated by antiphosphotyrosine staining. Significant suppression of membrane ruffles is also noted in the PP1-treated cells. (C) Effects of PP1 on the level of GTP-Rac in Y-27632–treated cells. The cells were cultured and treated as described above and then subjected to the pull-down assay for GTP-Rac. Control, cells treated with Y-27632 alone; PP1, cells treated with both Y-27632 and PP1. (D) Inhibition of LPA-induced membrane ruffles by expression of CasΔSD, a tyrosine phosphorylation-defective Cas mutant, in Y-27632–treated cells. Swiss 3T3 cells were transfected with 1 μg of pSSRα–CasΔSD and cultured as described in the legend to Fig. 2 A. The cells were then treated with 30 μM Y-27632 for 30 min and stimulated with 5 μM LPA for 5 min in the continued presence of Y-27632. The cells were fixed, and F-actin and tyrosine-phosphorylated proteins were stained as described above. The cells expressing CasΔSD were identified by HA tag staining and are indicated by arrows. Bars, 20 μm.

teins; one is mediated by ROCK and induces the phosphorylation of paxillin and FAK, and the other is ROCK independent and leads to the phosphorylation of Cas.

Tyrosine phosphorylation of Cas is required for LPA-induced membrane ruffling in Y-27632–treated cells

As previously reported (Sakai et al., 1994; Klinghoffer et al., 1999), p130Cas was tyrosine phosphorylated by the Src family of kinases. Therefore, we examined LPA-induced changes in Y-27632–treated cells in the presence of PP1, a specific inhibitor of Src family kinases (Hanke et al., 1996). Consistent with the previous report (Okuda et al., 1999), the treatment with PP1 significantly decreased the level of tyrosine phosphorylation of Cas (Fig. 4 A). Under these conditions, LPA-induced morphological changes were also inhibited (Fig. 4 B). The peripheral accumulation of F-actin was greatly suppressed, and F-actin was seen as disorganized tangles in the cytoplasm. Focal complexes beneath the membrane ruffles disappeared. These changes were observed in almost all PP1-treated cells. We also used the pull-down assay and have found that the level of GTP-Rac was significantly suppressed by the PP1 treatment (Fig. 4 C). These results suggest that the Cas phosphorylation leads to Rac activation and evokes membrane ruffles. To confirm this, we transfected 3T3 cells with CasΔSD. CasΔSD is a Cas mutant with a deletion of the tyrosine phosphorylation sites by Src kinase (Nakamoto et al., 1997), and overexpression of this mutant works as a dominant negative form in Cas signaling involving the phosphorylation (Klemke et al., 1998). As shown in Fig. 4 D, no LPA-induced membrane ruffling was seen, and the dot-like focal complexes disappeared in the Y-27632–treated cells expressing CasΔSD. F-actin was dispersed in the cytoplasm as observed in the cells expressing RacN17 (Fig. 2 A). This phenotype was observed in 48 cells out of 50 Cas‴ ΔSD-expressing cells in three independent experiments.

Overexpression of CrkII(R38K) and CrkII(W170K) inhibits LPA-induced membrane ruffling in Y-27632–treated cells

Tyrosine phosphorylation of Cas provides a binding site for Crk, which then binds DOCK180 to make a Cas–Crk–DOCK180 complex (O'Neill et al., 2000). Because DOCK180 is known as an activator for Rac (Kiyokawa et al., 1998), we examined the involvement of this complex formation in LPA-induced ruffling in our system. To this

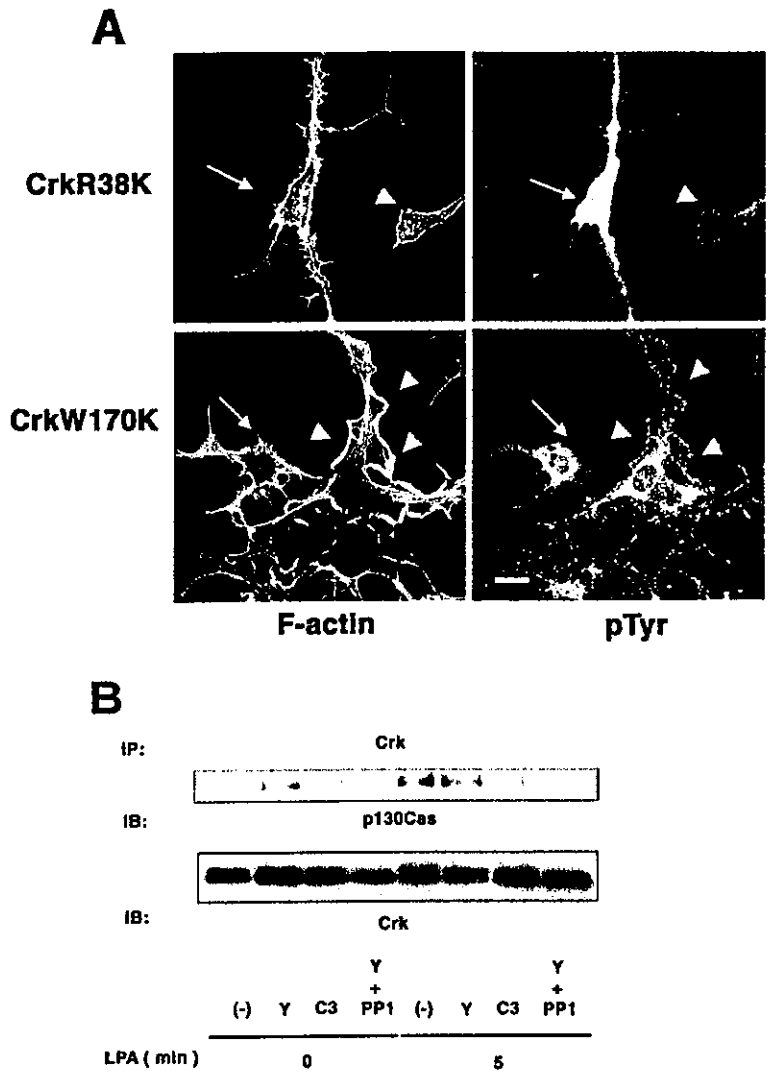

Figure 5. **Cas–Crk interaction in LPA-induced membrane ruffles in Y-27632–treated cells.** (A) Inhibition of the ruffle formation by expression of CrkII mutants. The cells were transfected either with 1 μg of pEEB–CrkII(R38K) and 0.1 μg of pEGFP–C1 (top) or with 1 μg of pEEB–CrkII(W170K) and 0.1 μg of pEGFP–C1 (bottom) and cultured as described in the legend to Fig. 2 A. The cells were then treated with 30 μM Y-27632 for 30 min and stimulated with 5 μM LPA for 5 min in the continued presence of Y-27632. The cells were fixed, and F-actin and tyrosine-phosphorylated proteins were stained as described above. The cells expressing each CrkII mutant were identified with anti-GFP staining and are indicated by arrows. Arrowheads indicate nontransfected cells. Note that the cell bodies of the cells expressing these CrkII mutants retracted, and the dot-like structure of tyrosine-phosphorylated proteins disappeared in the cell periphery. Bar, 20 μm. (B) Rho-dependent formation of the Cas–Crk complex in LPA-stimulated cells. Swiss 3T3 cells were cultured and treated with indicated reagents as described in the legends for Figs. 1 and 4. After stimulated with LPA for 0 and 5 min, the cells were lysed and subjected to immunoprecipitation with anti-Crk mAb. The immunoprecipitates were then analyzed by Western blot analysis with anti-Cas antibody.

purpose, we used two CrkII mutants. One is CrkII(R38K) that has a mutation in its SH2 region and is devoid of binding to Cas, and the other is CrkII(W170K) that has a mutation in its NH_2-terminal SH3 region and is devoid of binding to DOCK180 (Albert et al., 2000). Overexpression of either of the two mutants significantly blunted the LPA-induced responses in Y-27632–treated cells. The cells expressing the CrkII mutants did not spread and did not develop membrane ruffling (Fig. 5 A). The dot-like staining with antiphosphotyrosine antibody was not seen either in the cell periphery. Suppression of the membrane ruffles was found in all of the 20 CrkII(R38K) cells and 23 out of 24 CrkII(W170K) cells observed in three independent experiments. Together, these results suggest that Rac activation through Rho-dependent, ROCK-independent pathway in LPA-stimulated cells is mediated through Cas phosphorylation and the induction of the Cas–Crk–DOCK180 complex. Consistently, the Cas–Crk complex was formed in LPA-stimulated cells, and this formation was inhibited by treatment with either C3 exoenzyme or PP1 (Fig. 5 B).

Effects of mDia1 mutants on LPA-induced membrane ruffling in Y-27632–treated cells

The next question is the identity of the Rho effector mediating the Rho signaling to Cas phosphorylation. An obvious candidate is mDia1 because mDia1 cooperates with ROCK to induce stress fibers and focal adhesions (Watanabe et al., 1999). The interaction of mDia with Src was also reported (Tominaga et al., 2000). To identify the involvement of mDia1, we first prepared several truncation constructs of mDia1ΔN3. mDia1ΔN3 is a dominant active mutant that induces thin stress fibers and small focal adhesions in HeLa cells (Watanabe et al., 1999; Ishizaki et al., 2001). Mutants interfering with this phenotype are, therefore, expected to work as dominant negative forms in cells in physiological situations. Because mDia1ΔN3 consists of several domains and deletion of any of these domains leads to the loss of the active phenotype, we suspected that truncation mutants of this active mutant might compete with the full mDia1ΔN3 and interfere with its action. To test this possibility, we made mutants H + P, F2, CC, and mDia1ΔN3(HindIII) (Fig. 6 A). Among these mu-

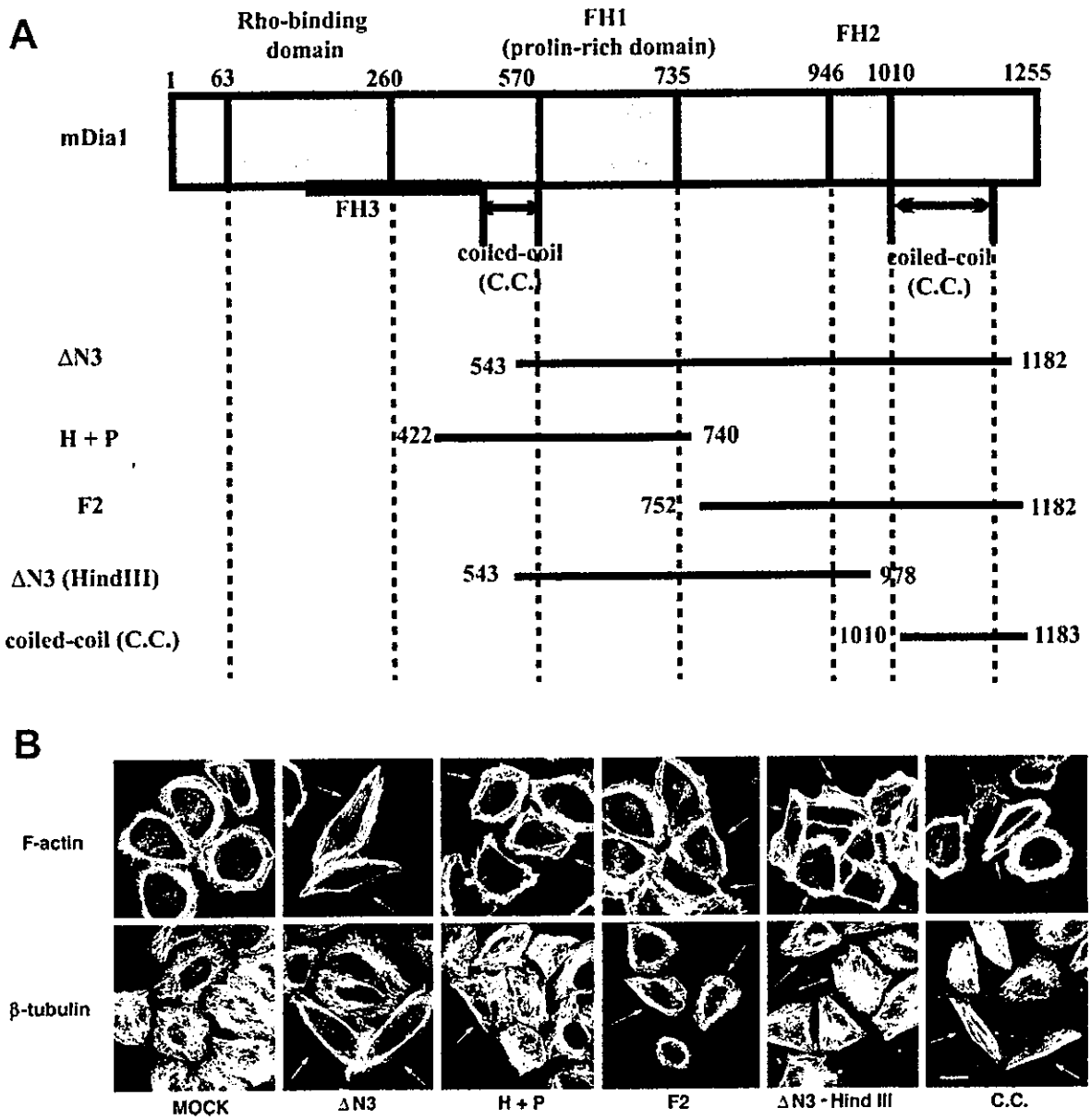

Figure 6. **Effects of various mDia1 fragments on the mDia1ΔN3 phenotype in HeLa cells.** (A) Schematic diagram of the structures of mDia1 and truncation mutants. The domain structure of mDia1 is shown above. The Rho-binding domain and the FH1 and FH2 regions are shown by hatched boxes. The FH3 region that partially overlaps with the Rho-binding domain and the two coiled-coil regions are indicated by a thick line and two-headed arrows, respectively. Truncation mutants, ΔN3, H + P, F2, ΔN3(HindIII) and CC are shown by the lines below. Numbers indicate the amino acid number at the NH_2 and COOH terminals of each protein and domain. (B and C) Effects of various fragments on the mDia1ΔN3 phenotype. HeLa cells were transfected with 0.2 μg of pFL–mDia1ΔN3 either alone or with 2 μg of pEGFP plasmid encoding either mDia1 H + P, F2, ΔN3(HindIII), or CC mutant. After the culture for 24 h, the cells were fixed and stained for F-actin (top) and β-tubulin (bottom) (B). Arrows indicate the cells expressing each construct. The ratios of the long versus short axis were measured in the cells expressing each construct and are shown (C). Note that expression of either H + P, F2, or ΔN3(HindIII) inhibits the cell elongation and the parallel alignment of F-actin bundles and MTs induced by mDia1ΔN3.

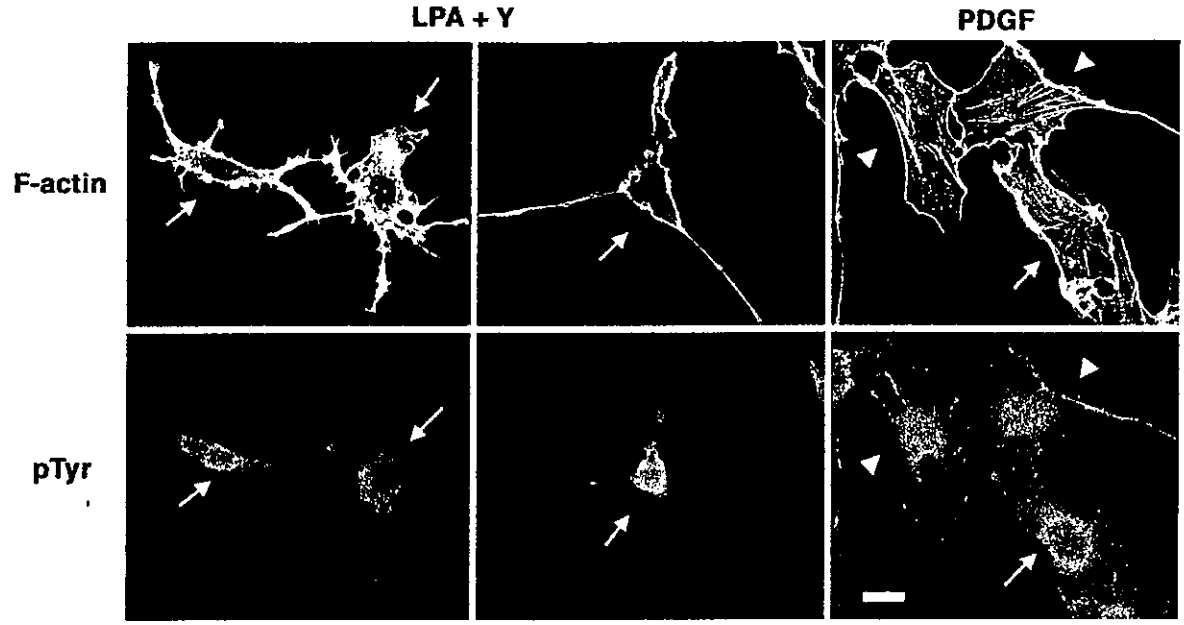

Figure 7. **Inhibition of LPA-induced membrane ruffles by expression of mDia1ΔN3(HindIII) in Y-27632–treated cells.** Swiss 3T3 cells were transfected with 1 μg of pEGFP plasmid encoding ΔN3(HindIII) and cultured as described in the legend to Fig. 2 A. The cells were treated with 30 μM Y-27632 for 30 min and then stimulated with 5 μM LPA for 5 min in the continued presence of Y-27632. Alternatively, the cells were stimulated with 5 ng/ml PDGF for 10 min without Y-27632 or LPA treatment. The cells were fixed, and F-actin and tyrosine-phosphorylated proteins were stained as described above. Left and middle panels show the cells stimulated with Y-27632 and LPA. The right panel shows cells stimulated with PDGF. Arrows indicate the cells expressing GFP–ΔN3–HindIII as identified by anti-GFP antibody staining. Arrowheads indicate nontransfected cells. Note that LPA-induced membrane ruffle formation is significantly suppressed by expression of mDia1–ΔN3(HindIII). Bar, 20 μm.

tants, H + P, F2, and mDia1ΔN3(HindIII) potently inhibited cell elongation and interfered with alignment of actin fibers and MTs induced by mDia1ΔN3 (Fig. 6, B and C). We then expressed these three mDia1 mutants individually in Swiss 3T3 cells and examined LPA-induced cell morphology in Y-27632–treated cells. Expression of mDia1ΔN3(HindIII) (Fig. 7) significantly inhibited LPA-induced membrane ruffling in Y-27632–treated cells. The dot-like focal complexes disappeared, and spreading was inhibited as seen in the cells expressing the Crk dominant negative mutants. This suppression was observed in 28 out of 30 cells expressing this construct. In contrast, the mDia1ΔN3(HindIII) expression did not inhibit the spreading and ruffle formation induced by PDGF. On the other hand, expression of either of the other two shorter mutants did not inhibit the LPA-induced membrane ruffle formation (unpublished data), suggesting that interference with endogenous mDia1 requires simultaneous blocking of various mDia1 domains. These results indicate that mDia1 works specifically as a switch of Rho activation to Rac activation.

Effects of MT disruption on Y-27632–induced membrane ruffling in serum-stimulated cells

Then, how does mDia1 mediate this action? We demonstrated that active mDia1 induces MT orientation to align actin fibers (Ishizaki et al., 2001). Kaverina et al. (1999) also suggested that MTs can promote cell protrusion by targeting focal adhesions and exerting relaxing effects. Therefore, we examined the effects of MT disruption by nocodazole on Y-27632–induced membrane ruffling. Because nocodazole treatment caused detachment of serum-starved cells from the dish, we added Y-27632 to cells cultured with serum and examined the effect of nocodazole. The addition of Y-27632 induced membrane ruffling also in serum-cultured cells, whereas the addition of nocodazole alone induced strong stress fibers as reported previously (Enomoto, 1996) (Fig. 8). On the other hand, combined addition of Y-27632 and nocodazole greatly attenuated stress fibers, indicating that Y-27632 sufficiently inhibited the ROCK activity also in these cells. Notably, this combined treatment also suppressed membrane ruffle formation, suggesting that membrane ruffle formation induced by Y-27632 depends on the activity of intact MTs. To test if disruption of microtubules could affect tyrosine phosphorylation of Cas, we analyzed tyrosine phosphorylation of Cas in control cells and cells treated with Y-27632 alone, nocodazole alone, or nocodazole and Y-27632. However, the Cas phosphorylation in these serum-maintained cells was low compared with the LPA-stimulated cells, and we could not detect any change in Cas phosphorylation among the groups of cells tested (unpublished data).

Discussion

ROCK and mDia1 antagonize in Rho-dependent Rac activation

In this study, by comparing the effects of C3 exoenzyme and Y-27632 on LPA-induced morphological change in serum-

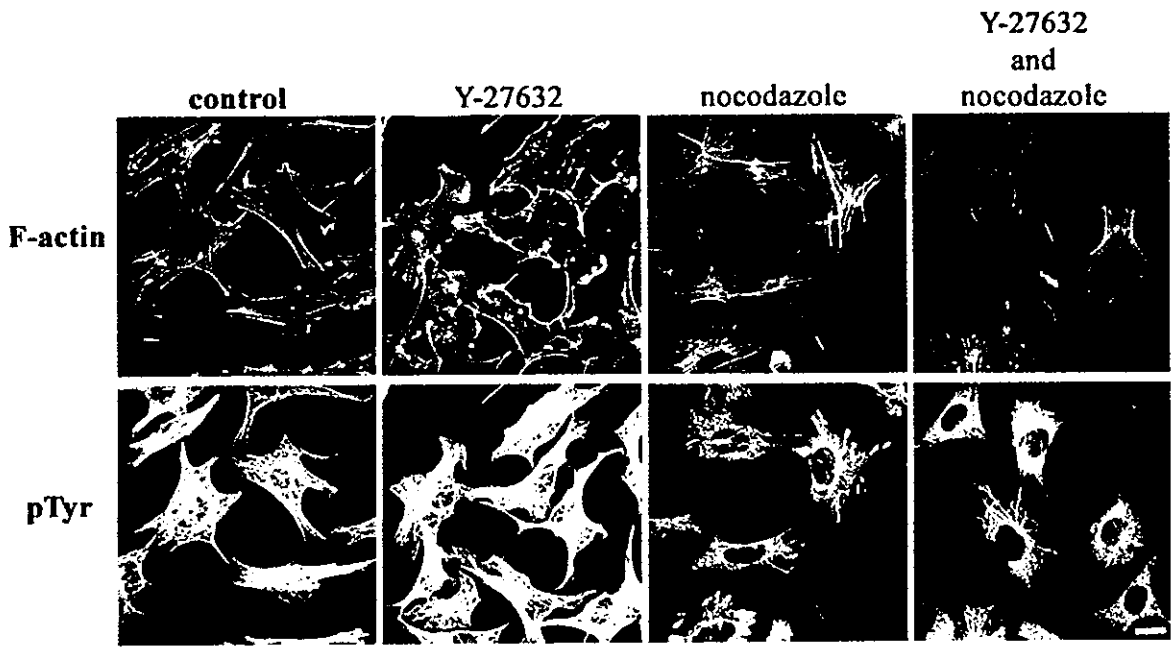

Figure 8. **Effects of nocodazole on Y-27632–induced membrane ruffles.** Swiss 3T3 cells were cultured in DME containing 10% FBS and treated with or without 30 μM Y-27632 in the presence or absence of 100 ng/ml nocodazole for 30 min. The cells were fixed and then stained for F-actin (top) and β-tubulin (bottom). Note that treatment of Y-27632 induced membrane ruffles at the tips of cells and that the addition of nocodazole inhibited the Y-27632–induced membrane ruffles. Bar, 20 μm.

starved Swiss 3T3 fibroblasts, we have first found that Rac is activated in a Rho-dependent manner, and this activation occurs when the ROCK pathway downstream of Rho is selectively inhibited. Induction of membrane ruffles by the Y-27632 treatment was reported previously by Rottner et al. (1999). These authors attributed this effect of ROCK inhibition to the presumed antagonism of Rho on Rac pathway originally observed in neuronal cells (Kozma et al., 1997; Van Leeuwen et al., 1997; Hirose et al., 1998). However, our findings that membrane ruffle formation and Rac activation were only seen in Y-27632–treated cells and not in cells treated with C3 exoenzyme argue against this hypothesis and suggest that a pathway mediated by other Rho effector(s) is responsible for this induction. Our subsequent analysis has indeed revealed that this Rac activation was evoked by the Rho-dependent tyrosine phosphorylation of Cas and the consequent formation of the Cas–Crk–DOCK180 complex. We have further found that the Y-27632–induced membrane ruffle formation was potently inhibited by expression of the dominant negative form of mDia1. mDia1 cooperates with ROCK downstream of Rho for correct induction of focal adhesions and stress fibers through MT alignment (Watanabe et al., 1999; Ishizaki et al., 2001). Binding of mDia1 to Src kinase and involvement of Src kinase in some mDia1-mediated actions was also reported (Tominaga et al., 2000). Src family kinases are also known to be responsible for integrin-dependent Cas phosphorylation (Klinghoffer et al., 1999). Consistently, the Y-27632–induced membrane ruffles in Swiss 3T3 cells were suppressed by disruption of MTs by nocodazole and inhibition of Src kinase by PP1. Together, these results suggest that mDia1 is an effector molecule mediating the Rho signal to Rac activation, and the ROCK pathway antagonizes this pathway of Rho-dependent Rac activation.

Then, how does the ROCK pathway antagonize the mDia1-mediated Rac activation? Because the level of GTP-Rac increases with ROCK inhibition (Fig. 2 B), the site of inhibition should be localized within the pathway from mDia1 to Rac activation by DOCK180. This inhibition site probably lies downstream of Cas because tyrosine phosphorylation of Cas was not enhanced by ROCK inhibition (Fig. 3, B and C). ROCK may interfere with this pathway through phosphorylation of paxillin. Yano et al. (2000) reported that paxillin α and Cas exert opposing effects on cell migration in a manner dependent on tyrosine phosphorylation of each protein. In this study, we have shown that tyrosine phosphorylation of paxillin is mediated by the ROCK pathway (Fig. 3, B and C).

Tyrosine phosphorylation of focal adhesion proteins occurs in many types of cells under a variety of stimuli, which utilize different signaling pathways. Therefore, our present findings naturally cannot be applied to every cell type. For example, in vascular endothelial cells stimulated with sphingosine-1 phosphate, tyrosine phosphorylation of Cas occurs in a manner not dependent on Rho (Ohmori et al., 2001), whereas similar to our finding bombesin induces Cas phosphorylation in a Rho-dependent, Y-27632–insensitive manner in Swiss 3T3 cells (Sinnett-Smith et al., 2001).

Implication of the dichotomy of the Rho signaling in the cell to substrate adhesion

The above findings suggest that two Rho effectors act differently downstream of Rho in the regulation of cell to sub-

strate adhesion and actin reorganization. Then, what is the implication of this dichotomy of the Rho signaling? The signaling and cytoskeletal dynamics that occur in cell spreading and adhesion as we analyzed in this study are generally thought to mimic events in migrating cells. Indeed, the bimodal Rho actions in migrating cells were suggested by an in vitro wound healing experiment using REF cells. Nobes and Hall (1999) microinjected two doses of C3 exoenzyme into migrating REF cells and found that the low dose that was sufficient to abolish stress fibers and focal adhesions did not affect cell migration, whereas the high dose completely inhibited cell migration. They also found that Y-27632 treatment accelerated the migration of the cells. The latter finding appears to be consistent with our current findings that treatment with Y-27632 and not C3 exoenzyme induces membrane ruffles. We have also found that treatment with Y-27632 and not C3 exoenzyme enhances the LPA-induced migration of Swiss 3T3 cells in the transwell assay (unpublished data). These results together with the above findings with the different doses of C3 exoenzyme suggest that the ROCK and mDia pathways differ in their sensitivities to C3 exoenzyme, the former being preferentially affected by the low dose and the latter becoming affected by the high dose. Such different sensitivities to C3 exoenzyme may indicate that activation of these two Rho pathways depend on the level of GTP-Rho in the cell, the low level being sufficient for the mDia1 pathway and the high level being required for the ROCK pathway. The level of GTP-Rho in the cell is regulated by both guanine nucleotide exchange factor and GTPase-activating protein (GAP) selective to this GTPase. Recently, Arthur and Burridge (2001) reported that the overexpression of wild-type p190RhoGAP facilitates spreading and migration of fibroblasts, whereas that of dominant negative p190RhoGAP (RA) inhibits these processes and that these phenotypes correlated with the low and high GTP-Rho levels, respectively. The phenotype induced by wild-type p190RhoGAP are similar to those of Y-27632–treated cells we described here, suggesting that p190RhoGAP may decrease the GTP-Rho level to interfere with the ROCK pathway. Consistently, they reported that the phenotype induced by the dominant negative p190RhoGAP (RA) mutant was reversed by the low dose of C3 exoenzyme. These results are consistent with a widely held view that the basal Rho activity is essential for cell migration and spreading (Nobes and Hall, 1999; Arthur and Burridge, 2001). Interestingly, the activity of p190RhoGAP is regulated through phosphorylation by c-Src that is activated in an integrin-dependent manner (Arthur et al., 2000). mDia1 may mediate this recruitment of Src to focal adhesions.

The dichotomy of the Rho signaling in the cell to substrate adhesion may also be important in the regulation of the cell cycle by Rho. The G1 to S phase progression of Swiss 3T3 cells is inhibited by C3 exoenzyme but not by Y-27632 (Yamamoto et al., 1993; Ishizaki et al., 2000). It is interesting to examine whether the mDia1-mediated signaling we described here works in this process. Another process where the mDia1-mediated signaling may work is Ras-induced cell transformation. Although Rho signaling is essential in Ras-induced transformation (Qiu et al., 1995), neither stress fibers nor focal adhesions are found in Ras-transformed cells, indicating that the Rho signaling is somehow modified in these cells. Sahai et al. (2001) reported that ROCK is down-regulated by both decreased expression and the cytoskeletal sequestration, whereas the level of GTP-Rho is elevated in Ras-transformed cells. These results indicate that the Rho signaling other than the ROCK pathway is important in the Ras-induced malignant transformation.

Rho-dependent Rac activation and the spatiotemporal control of cell migration

Cell migration is presumably performed by concerted formation of filopodia, lamellipodia, and actomyosin contraction each induced by the Rho family GTPases, Cdc42, Rac, and Rho (Mitchison and Cramer, 1996). Previously, the hierarchical activation of Cdc42 to Rac and then to Rho was shown and suggested to work in a cascade in cell migration (Chant and Stowers, 1995). However, these studies did not provide any information on activation of Rac or Cdc42 by Rho, which is essential to resume the migration cycle. Our present findings have for the first time demonstrated that the Rho signaling has a built-in switch for Rac activation. We have found that this switch is mediated by mDia1 and inhibited by ROCK. In this respect, it is interesting that mDia1 recruits MT ends to focal adhesions (Ishizaki et al., 2001) and that targeting of focal adhesions by MTs appears to inhibit the ROCK activity there (Kaverina et al., 1999). Together, these results suggest that the Rho-dependent Rac activation may be switched on in a positive feedback manner by mDia1. In migrating cells, signaling pathways of these Rho GTPases are regulated not only temporally but also spatially. mDia1 was previously shown to be localized in membrane ruffles of motile cells (Watanabe et al., 1997). On the other hand, recent studies suggest that the ROCK activity is required in the tail retraction of migrating monocytes and neutrophils (Worthylake et al., 2001). Thus, the two Rho signaling pathways may operate differently in space in migrating cells, the mDia1 and ROCK pathways preferentially in the front and the rear, respectively.

Materials and methods

Materials

LPA, nocodazole, anti-FLAG monoclonal antibody (M2), and anti-β-tubulin antibody (TUB.2.1) were purchased from Sigma-Aldrich. Antiphosphotyrosine polyclonal antibody (PY20) and monoclonal antibody (4G10) were purchased from Zymed Laboratories and Upstate Biotechnology, respectively. Clone 2A7 and clone 77 anti-FAK monoclonal antibodies were purchased from Upstate Biotechnology and Transduction Laboratory, respectively. Antipaxillin monoclonal antibody was purchased from Zymed Laboratories. PDGF-BB, anti-Rac1, and anti-Crk antibodies were purchased from Upstate Biotechnology. Anti-p130Cas polyclonal antibody was reported previously (Nakamoto et al., 1997). Y-27632, a ROCK inhibitor, was supplied by Mitsubishi Pharma. *Botulinum* C3 exoenzyme was purified as described (Morii and Narumiya, 1995). GST-PAK CRIB protein was prepared as described previously (Matsuo et al., 2002).

Plasmids

pE-green fluorescent protein (GFP)-C1 was purchased from CLONTECH Laboratories, Inc. pSSRα-p130CasΔSD, pEEB-CrkII(R38K), and pEEB-CrkII(W170K) were described previously (Nakamoto et al., 1997; Albert et al., 2000). pFL-mDia1ΔN3, pEGFP-mDia1-F2, and pEGFP-mDia1-H + P were constructed as described previously (Watanabe et al., 1999; Ishizaki et al., 2001). For construction of pEGFP-mDia1-CC, PCR was performed with

pFL-mDia1-Full (Watanabe et al., 1999) as a template using a forward primer (5'-TTCCTCGAGGCCTTCGGCCTCGCCTC-3') and a reverse primer (5'-TTCGGATCCGTCCATCACACCTGTCTCATC-3'). The product was digested with XhoI and BamHI and inserted into a XhoI-BamHI fragment of pEGFP-C1. For construction of pEGFP-mDia1ΔN3(HindIII), pGEX-4T-mDia1ΔN3 was digested with BglII and HindIII. The insert was ligated with a BglII-HindIII fragment of pEGFP-C1. pCMV5-FLAG-N19Rac was described previously (Hirose et al., 1998). pEGFP actin was constructed as follows. Mouse β-actin cDNA was amplified from adult mouse brain mRNA using reverse transcriptase-PCR. NcoI-FSPI fragment was inserted between Asp718I and BamHI sites in pEGFP-C1 with the blunt-end ligation. The resultant plasmid contains mouse β-actin ORF fused to the COOH terminus of EGFP in frame with the linker of 17 amino acids.

Cell culture and transfection

For LPA stimulation of nontransfected cells, Swiss 3T3 cells were plated at densities of 2×10^4 and 2×10^5 cells per 35- and 60-mm dish for immunofluorescence study or immunoprecipitation assay, respectively, and cultured in DME containing 10% FCS for 3 d. The cells were washed twice with Ca^{2+}- and Mg^{2+}-free PBS(−) and cultured in serum-free DME for 24 h. During this period, the cells were without treatment or treated either with 30 μg/ml C3 exoenzyme all through the culture of 4 d or with 30 μM Y-27632 for the last 30 min. The cells were then stimulated with 5 μM LPA for the indicated times in the continued presence of C3 coenzyme or Y-27632. The cells were either fixed or lysed as described below. For transfection, Swiss 3T3 cells were plated on a cover glass at a density of 2×10^4 cells per 22-mm dish and cultured in DME containing 10% FCS for 24 h. The cells were washed with PBS(−) once and incubated with the indicated amounts of plasmid DNA(s) mixed with 1 μl of Lipofectamine 2000 for 3 h in 1 ml of OPTI-MEM (GIBCO BRL). The medium was replaced with DME containing 10% FCS, and the cells were cultured for 18 h. The cells were then cultured in serum-free DME for 24 h and treated with Y-27632 for the last 30 min. The cells were stimulated with 5 μM LPA for the indicated times in the continued presence of Y-27632. The cells were fixed and stained as described below. As indicated, PDGF stimulation on nontransfected or transfected cells was performed at 5 ng/ml concentration for 10 min.

HeLa cells were plated on a cover glass at a density of 5×10^4 cells per 35-mm dish and cultured in DME containing 10% FCS for 24 h. The cells were washed once and incubated with 0.2 μg of pFL-mDia1ΔN3 with or without 2 μg of the pEGFP plasmid encoding each mDia1 mutant mixed with 4 μl of Lipofectamine (GIBCO BRL) for 3 h in 1 ml of OPTI-MEM (GIBCO BRL). The medium was replaced with DME containing 10% FCS, and the cells were cultured for 18 h. The cells were then fixed and stained.

Immunofluorescence study

The cells were washed once with PBS(−) and fixed as follows. HeLa cells were fixed with 4% formaldehyde as described previously (Ishizaki et al., 2001). Swiss 3T3 cells were fixed first for 1 min with 4% formaldehyde and 0.1% Triton X-100 in PBS and then for 15 min with 4% formaldehyde alone in PBS. Both lines of the cells were permeabilized by washing in PBS(−) containing 0.1% Triton X-100 for 5 min and incubated with PBS(−) containing 3% BSA for 1 h at room temperature. Primary antibodies were diluted in PBS(−) containing 1% BSA and included the antibodies against pTyr (1:100), β-tubulin (1: 200), the Flag tag (1:100), and the GFP tag (1:100). F-actin was always stained with Texas red phalloidin (Molecular Probes). In double staining for F-actin and phosphotyrosine, Alexa Fluor 488–conjugated goat anti–mouse IgG (H + L) (Molecular Probes) was used as the secondary antibody. In triple staining for F-actin, phosphotyrosine, and tag epitopes, Alexa Fluor 488–conjugated goat anti–mouse IgG (H + L) was used for detection of the signal of the tag epitope, and Alexa Fluor 633–conjugated goat anti–rabbit IgG (H + L) (Molecular Probes) was used for detection of the signal of rabbit polyclonal antibody to phosphotyrosine. Alexa Fluor 594–conjugated goat anti–rabbit IgG (H + L) (Molecular Probes) was used as the secondary antibody for detection of MTs. Optical sections of 0.3-μm thickness were obtained from the bottom with a Bio-Rad Laboratories MRC1024 Confocal Imaging System, and built-up images were constructed.

Videomicroscopy

Swiss 3T3 cells were seeded at a density of 2×10^4 per dish in a 35-mm glass-bottom dish (Matsunami Glass) and cultured for 24 h. The cells were transfected with 1 μg of pEGFP actin as described above and then maintained for 3 d. The cells were starved in serum-free DME for 24 h and treated with 30 μM Y-27632 for the last 30 min. The dish was transferred to a temperature-controlled ZEISS CO_2 incubator attached to the microscope stage. 5 μM LPA was then added, and the cell movement was monitored at 37°C in 5% CO_2 for 90 min using a ZEISS confocal laser scanning unit (LSM 510-V2.5). Three successive optical sections of 0.6-μm thickness were obtained from the bottom every 90 s, and built-up images were constructed.

Western blot analysis and immunoprecipitation

Swiss 3T3 cells were washed once with ice-cold PBS(−) and lysed on ice for 5 min with modified RIPA buffer containing 50 mM Tris-HCl, pH 7.5, 150 mM NaCl, 1% NP-40, 0.25% SDS, 0.25% sodium deoxycholate, 1 mM sodium fluoride, 1 mM sodium orthovanadate, 1 μg/ml leupeptin, 1 μg/ml aprotinin, 1 μg/ml pepstatin, 1 mM EGTA, and 1 mM PMSF. The samples were centrifuged at 12,000 *g* for 20 min, and the supernatant was collected as the cell lysates. Protein concentration of the lysates was determined by the Lowry method. For Western blot analysis using the total cell lysates, one fifth volume of the 5× Laemmli sample buffer was added to the lysates. The mixtures were boiled for 5 min and subjected to SDS-PAGE and Western blot analysis using antiphosphotyrosine antibody (4G10) as described (Needham and Rozengurt, 1998). For immunoprecipitation, 50 μg of each cell lysate was incubated with 1 μg of either anti-p130Cas polyclonal antibody, anti-FAK monoclonal antibody, antipaxillin monoclonal antibody, or antiphosphotyrosine monoclonal antibody (4G10). 30 μl of either protein A–Sepharose (for precipitation of anti-p130Cas antibody complex only) or protein G–Sepharose (Amasham Pharmacia Biotech) were then added, and incubation was performed for 3 h at 4°C. The Sepharose beads were washed three times with the lysis buffer and suspended with an equal volume of 2× Laemmli sample buffer. The suspensions were boiled, and the extracts were subjected to Western blot analysis using the indicated antibodies. Immunoprecipitation of Crk was performed as described (Gu et al., 2001).

Pull-down assay

Swiss 3T3 cells were plated at a density of 5×10^5 cells per 10-cm dish. Culture, treatment with Y-27632, or C3 exoenzyme and LPA stimulation were performed as described above. The cells were washed once with ice-cold PBS(−) and lysed in the pull-down lysis buffer containing 50 mM Tris-HCl, pH 7.5, 100 mM NaCl, 2 mM $MgCl_2$, 10% glycerol, 1% NP-40, 1 μg/ml leupeptin, 1 μg/ml aprotinin, 1 μg/ml pepstatin, 1 mM sodium fluoride, 1 mM EGTA, and 1 mM PMSF. The samples were centrifuged at 12,000 *g* for 20 min, and the supernatants were saved as the cell lysates. After protein concentration was determined by the Lowry method, 200 μg protein of cell lysate was incubated with 20 μg protein of GST-PAK CRIB immobilized on glutathione–Sepharose 4B beads (Amersham Pharmacia Biotech) for 1 h at 4°C. Beads were washed three times with the pull-down buffer, and bound GTP-Rac1 was detected by Western blot with anti-Rac1 antibody.

Online supplemental materials

Fig. S1, showing the effect of Y-27632 on morphology of C3 exoenzyme-treated cells, Fig. S2, showing the effect of PDGF on morphology of C3 exoenzyme-treated cells, and the video, showing LPA-induced membrane ruffling of Y-27632–treated cells, are available online at http://www.jcb.org/cgi/content/full/jcb.200112107/DC1.

We thank Dr. M. Hoshino for providing pGEX-PAK-CRIB, Dr. H. Bito for useful advice, and Ms. K. Nonomura, H. Nose, and T. Arai for assistance.

This work was supported in part by a grant in aid for Specially Promoted Research from the Ministry of Education, Culture, Sports Science and Technology of Japan and a grant from the Organization for Pharmaceutical Safety and Research.

Submitted: 20 December 2001
Revised: 12 April 2002
Accepted: 12 April 2002

References

Albert, M.L., J.I. Kim, and R.B. Birge. 2000. $\alpha_v\beta_5$ integrin recruits the CrkII-Dock180-rac1 complex for phagocytosis of apoptotic cells. *Nat. Cell Biol.* 2:899–905.

Allen, W.E., D. Zicha, A.J. Ridly, and G.E. Jones. 1998. A role for Cdc42 in macrophage chemotaxis. *J. Cell Biol.* 141:1147–1157.

Amano, M., K. Chihara, K. Kimura, Y. Fukata, N. Nakamura, Y. Matsuura, and K. Kaibuchi. 1997. Formation of actin stress fibers and focal adhesions enhanced by Rho-kinase. *Science.* 275:1308–1311.

Arthur, W.T., and K. Burridge. 2001. RhoA inactivation by p190RhoGAP regulates cell spreading and migration by promoting membrane protrusion and polarity. *Mol. Biol. Cell.* 12:2711–2720.

Arthur, W.T., L.A. Petch, and K. Burridge. 2000. Integrin engagement suppresses RhoA activity via a c-Src-dependent mechanism. *Curr. Biol.* 10:719–722.

Chant, J., and L. Stowers. 1995. GTPase cascades choreographing cellular behavior: movement, morphogenesis, and more. *Cell.* 81:1–4.

Enomoto, T. 1996. MT disruption induces the formation of actin stress fibers and focal adhesions in cultured cells: possible involvement of the Rho signal cascade. *Cell Struct. Funct.* 21:317–326.

Gu, J., Y. Sumida, N. Sanzen, and K. Sekiguchi. 2001. Laminin-10/11 and fibronectin differentially regulate integrin-dependent Rho and Rac activation via p130^{Cas}-CrkII-DOCK180 pathway. *J. Biol. Chem.* 276:27090–27097.

Hall, A. 1998. Rho GTPases and the actin cytoskeleton. *Science.* 279:509–514.

Hanke, J.H., J.P. Gardner, R.L. Dow, P.S. Changelian, W.H. Brissette, E.J. Weringer, B.A. Pollok, and P.A. Connelly. 1996. Discovery of a novel, potent, and Src family-selective tyrosine kinase inhibitor. Study of Lck- and Fyn-dependent T cell activation. *J. Biol. Chem.* 271:695–701.

Hirose, M., T. Ishizaki, N. Watanabe, M. Uehata, O. Kranenburg, W.H. Moolenaar, F. Matsumura, M. Maekawa, H. Bito, and S. Narumiya. 1998. Molecular dissection of the Rho-associated protein kinase (p160ROCK)-regulated neurite remodeling in neuroblastoma N1E-115 cells. *J. Cell Biol.* 141:1625–1636.

Horwitz, A.R., and J.T. Parsons. 1999. Cell migration—movin' on. *Science.* 286: 1102–1103.

Ishizaki, T., M. Naito, K. Fujisawa, M. Maekawa, N. Watanabe, Y. Saito, and S. Narumiya. 1997. p160ROCK, a Rho-associated coiled-coil forming protein kinase, works downstream of Rho and induces focal adhesions. *FEBS Lett.* 404:118–124.

Ishizaki, T., M. Uehata, I. Tamechika, J. Keel, K. Nonomura, M. Maekawa, and S. Narumiya. 2000. Pharmacological properties of Y-27632, a specific inhibitor of rho-associated kinases. *Mol. Pharmacol.* 57:976–983.

Ishizaki, T., Y. Morishima, M. Okamoto, T. Furuyashiki, T. Kato, and S. Narumiya. 2001. Coordination of MTs and the actin cytoskeleton by the Rho effector mDia1. *Nat. Cell Biol.* 3:8–14.

Kaverina, I., O. Krylyshkina, and J.V. Small. 1999. MT targeting of substrate contacts promotes their relaxation and dissociation. *J. Cell Biol.* 146:1033–1044.

Kiyokawa, E., Y. Hashimoto, S. Kobayashi, H. Sugimura, T. Kurata, and M. Matsuda. 1998. Activation of Rac1 by a Crk SH3-binding protein, DOCK180. *Genes Dev.* 12:3331–3336.

Klemke, R.L., J. Leng, R. Molander, P.C. Brooks, K. Vuori, and D.A. Cheresh. 1998. CAS/Crk coupling serves as a "molecular switch" for induction of cell migration. *J. Cell Biol.* 140:961–972.

Klinghoffer, R.A., C. Sachsenmaier, J.A. Cooper, and P. Soriano. 1999. Src family kinases are required for integrin but not PDGFR signal transduction. *EMBO J.* 18:2459–2471.

Kozma, R., S. Sarner, S. Ahmed, and L. Lim. 1997. Rho family GTPases and neuronal growth cone remodeling: relationship between increased complexity induced by Cdc42Hs, Rac1, and acetylcholine and collapse induced by RhoA and lysophosphatidic acid. *Mol. Cell. Biol.* 17:1201–1211.

Kumagai, N., N. Morii, K. Fujisawa, Y. Nemoto, and S. Narumiya. 1993. ADP-ribosylation of rho p21 inhibits lysophosphatidic acid-induced protein tyrosine phosphorylation and phosphatidylinositol 3-kinase activation in cultured Swiss 3T3 cells. *J. Biol. Chem.* 268:24535–24538.

Leung, T., X.Q. Chen, E. Manser, and L. Lim. 1996. The p160 RhoA-binding kinase ROK alpha is a member of a kinase family and is involved in the reorganization of the cytoskeleton. *Mol. Cell. Biol.* 16:5313–5327.

Matsuo, N., M. Hoshino, M. Yoshizawa, and Y. Nabeshima. 2002. Characterization of STEF, a guanine nucleotide exchange factor for Rac1, required for neurite growth. *J. Biol. Chem.* 277:2860–2868.

Mitchison, T.J., and L.P. Cramer. 1996. Actin-based cell motility and cell locomotion. *Cell.* 84:371–379.

Morii, N., and S. Narumiya. 1995. Preparation of native and recombinant *Clostridium botulinum* C3 ADP-ribosyltransferase and identification of Rho proteins by ADP-ribosylation. *Methods Enzymol.* 256:196–206.

Nakamoto, T., R. Sakai, H. Honda, S. Ogawa, H. Ueno, T. Suzuki, S. Aizawa, Y. Yazaki, and H. Hirai. 1997. Requirements for localization of p130cas to focal adhesions. *Mol. Cell. Biol.* 17:3884–3897.

Narumiya, S. 1996. The small GTPase Rho: cellular functions and signal transduction. *J. Biochem. (Tokyo).* 120:215–228.

Needham, L.K., and E. Rozengurt. 1998. Gα12 and Gα13 stimulate Rho-dependent tyrosine phosphorylation of focal adhesion kinase, paxilin, and p130 Crk-associated substrate. *J. Biol. Chem.* 273:14626–14632.

Nobes, C.D., and A. Hall. 1999. Rho GTPases control polarity, protrusion, and adhesion during cell movement. *J. Cell Biol.* 144:1235–1244.

Ohmori, T., Y. Yatomi, H. Okamoto, Y. Miura, G. Rile, K. Satoh, and Y. Ozaki. 2001. Gi-mediated Cas tyrosine phosphorylation in vascular endothelial cells stimulated with sphingosine 1-phosphate: possible involvement in cell motility enhancement in cooperation with Rho-mediated pathways. *J. Biol. Chem.* 276:5274–5280.

Okuda, M., M. Takahashi, J. Suehiro, C.E. Murry, O. Traub, H. Kawakatsu, and B.C. Berk. 1999. Shear stress stimulation of p130^{cas} tyrosine phosphorylation requires calcium-dependent c-Src activation. *J. Biol. Chem.* 274:26801–26809.

O'Neill, GM., A.J. Fashena, and E.A. Golemis. 2000. Integrin signalling: a new Cas(t) of characters enters the stage. *Trends Cell Biol.* 10:111–119.

Qiu, R.G., J. Chen, F. McCormick, and M. Symons. 1995. A role for Rho in Ras transformation. *Proc. Natl. Acad. Sci. USA.* 92:11781–11785.

Rankin, S., N. Morii, S. Narumiya, and E. Rozengurt. 1994. Botulinum C3 exoenzyme blocks the tyrosine phosphorylation of p125FAK and paxillin induced by bombesin and endothelin. *FEBS Lett.* 354:315–319.

Ridley, A.J., and A. Hall. 1992. The small GTP-binding protein rho regulates the assembly and focal adhesions and actin stress fibers in response to growth factors. *Cell.* 70:389–399.

Rottner, K., A. Hall, and J.V. Small. 1999. Interplay between Rac and Rho in the control of substrate contact dynamics. *Curr. Biol.* 9:640–648.

Sahai, E., M.F. Olson, and C.J. Marshall. 2001. Cross-talk between Ras and Rho signalling pathways in transformation favours proliferation and increased motility. *EMBO J.* 20:755–766.

Sakai, R., A. Iwamatsu, N. Hirano, S. Ogawa, T. Tanaka, H. Mano, Y. Yazaki, and H. Hirai. 1994. A novel signaling molecule, p130, forms stable complexes in vivo with v-Crk and v-Src in a tyrosine phosphorylation-dependent manner. *EMBO J.* 13:3748–3756.

Sander, E.E., S. van Delft, J.P. ten Klooster, T. Reid, R.A. van der Kammen, F. Michiels, and J.G. Collard. 1998. Matrix-dependent Tiam1/Rac signaling in epithelial cells promotes either cell-cell adhesion or cell migration and is regulated by phosphatidylinositol 3-kinase. *J. Cell Biol.* 143:1385–1398.

Schmitz, A.A., E.E. Govek, B. Bottner, and L. Van Aelst. 2000. Rho GTPases: signaling, migration, and invasion. *Exp. Cell Res.* 261:1–12.

Sinnett-Smith, J., J.A. Lunn, D. Leopoldt, and E. Rozengurt. 2001. Y-27632, an inhibitor of Rho-associated kinases, prevents tyrosine phosphorylation of focal adhesion kinase and paxillin induced by bombesin: dissociation from tyrosine phosphorylation of p130^{CAS}. *Exp. Cell Res.* 266:292–302.

Tominaga, T., E. Sahai, P. Chardin, F. McCormick, S.A. Courtneidge, and A.S. Alberts. 2000. Diaphanous-related formins bridge Rho GTPase and Src tyrosine kinase signaling. *Mol. Cell.* 5:13–25.

Uehata, M., T. Ishizaki, H. Satoh, T. Ono, T. Kawahara, T. Morishita, H. Tamakawa, K. Yamagami, J. Inui, M. Maekawa, and S. Narumiya. 1997. Calcium sensitization of smooth muscle mediated by a Rho-associated protein kinase in hypertension. *Nature.* 389:990–994.

Van Leeuwen, F.N., H.E.T. Kain, R.A. van de Kammen, F. Michiels, O.W. Kranenburg, and J.C. Collard. 1997. The guanine nucleotide exchange factor Tiam 1 affects neuronal morphology: opposing roles for the small GTPases Rac and Rho. *J. Cell Biol.* 139:797–807.

Watanabe, N., P. Madaule, T. Reid, T. Ishizaki, G. Watanabe, A. Kakizuka, Y. Saito, K. Nakao, B.M. Jockusch, and S. Narumiya. 1997. p140mDia, a mammalian homolog of *Drosophila diaphanous*, is a target protein for Rho small GTPase and is a ligand for profilin. *EMBO J.* 16:3044–3056.

Watanabe, N., T. Kato, A. Fujita, T. Ishizaki, and S. Narumiya. 1999. Cooperation between mDia1 and ROCK in Rho-induced actin reorganization. *Nat. Cell Biol.* 1:136–143.

Worthylake, R.A., S. Lemoine, J.M. Watson, and K. Burridge. 2001. RhoA is required for monocyte tail retraction during transendothelial migration. *J. Cell Biol.* 154:147–160.

Yamamoto, M., N. Marui, T. Sakai, N. Morii, S. Kozaki, K. Ikai, S. Imamura, and S. Narumiya. 1993. ADP-ribosylation of the rhoA gene product by botulinum C3 exoenzyme causes Swiss 3T3 cells to accumulate in the G1 phase of the cell cycle. *Oncogene.* 8:1449–1455.

Yano, H., H. Uchida, T. Iwasaki, M. Mukai, H. Akedo, K. Nakamura, S. Hashimoto, and H. Sabe. 2000. Paxillin α and Crk-associated substrate exert opposing effects on cell migration and contact inhibition of growth through tyrosine phosphorylation. *Proc. Natl. Acad. Sci. USA.* 97:9076–9081.

Article

The Rho-associated protein kinase p160ROCK is required for centrosome positioning

Véronique Chevrier,[1] Matthieu Piel,[2] Nora Collomb,[1] Yasmina Saoudi,[1] Ronald Frank,[3] Michel Paintrand,[1] Shuh Narumiya,[4] Michel Bornens,[2] and Didier Job[1]

[1]Institut National de la Santé et de la Recherche Medicale U366, Département de Biologie Moléculaire et Structurale/Cytosquelette, Commissariat à l'Energie Atomique, de Grenoble, 38054 Grenoble Cedex 9, France
[2]Institut Curie, Section Recherche, UMR 144 du Centre National de la Recherche Scientifique, 75248 Paris Cedex 05, France
[3]AG Molecular Recognition, Gesellschaft für Biotechnologische Forschung, D-38124 Braunschweig, Germany
[4]Department of Pharmacology, Kyoto University Faculty of Medicine, Sako-ku, Kyoto 606, Japan

The p160–Rho-associated coiled-coil–containing protein kinase (ROCK) is identified as a new centrosomal component. Using immunofluorescence with a variety of p160ROCK antibodies, immuno EM, and depletion with RNA interference, p160ROCK is principally bound to the mother centriole (MC) and an intercentriolar linker. Inhibition of p160ROCK provoked centrosome splitting in G1 with the MC, which is normally positioned at the cell center and shows little motion during G1, displaying wide excursions around the cell periphery, similar to its migration toward the midbody during cytokinesis. p160ROCK inhibition late after anaphase in mitosis triggered MC migration to the midbody followed by completion of cell division. Thus, p160ROCK is required for centrosome positioning and centrosome-dependent exit from mitosis.

Introduction

Centrosomes, the major microtubule-organizing centers in mammalian cells, are complex organelles, comprising two centrioles associated by the pericentriolar matrix. Centrosomes are involved in both cell motility and cell division. In migrating cells, centrosome positioning is involved in the stabilization of pseudopodia (Ueda et al., 1997). Centrosomes are subject to important structural modifications during the cell cycle, including duplication, maturation, and separation (for reviews see Andersen, 1999; Tassin and Bornens, 1999; Hinchcliffe and Sluder, 2001).

Recent studies have revealed differential behavior of the two centrioles (Piel et al., 2000, 2001). In G1 cells, although the mother centriole (MC) stays close to the cell center, the daughter centriole (DC) shows wide excursions throughout the cell cytoplasm. The MC is responsible for the formation of a microtubule aster, and this is probably the basis for its positioning at the cell center (Holy et al., 1997). In contrast, the DC nucleates microtubules that are released and migrate toward the cell periphery (Piel et al., 2000). This combination of a centered, microtubule-anchoring MC and of a mobile, microtubule-releasing DC could be important for directional cell motility. In addition, centrosome organization and motions are apparently crucial for the completion of cytokinesis. The separation of daughter cells at the end of mitosis is apparently controlled by a migration of the MC toward the midbody (Piel et al., 2001).

Some of the factors important for the control of centrosome organization and centrosome behavior have been identified. The ability of the MC to generate microtubule asters is attributable to specific features of its associated pericentriolar material (PCM),* which contains the microtubule-anchoring protein ninein (Mogensen et al., 2000; Piel et al., 2000). The relative position of the two centrioles and the centrosome movements within cells are dependent on both microtubule and microfilaments organization (Euteneuer and Schliwa, 1985; Schliwa et al., 1999). Centrosome cohesion is affected by the kinase Nek2 (Fry et al., 1998a,b; Mayor et al., 2000; Meraldi and Nigg, 2001). The identification of additional centrosome regulators may arise from an inventory of the centrosome components. To identify PCM components, we have previously developed monoclonal antibodies

Address correspondence to Didier Job, INSERM U366, DBMS/CS, CEA de Grenoble, 17 Rue des Martyrs, 38054 Grenoble Cedex 9, France. Tel.: 33-04-38-78-51-00. Fax: 33-04-38-78-50-57. E-mail: djob@cea.fr

V. Chevrier and M. Piel contributed equally to this work.

Key words: centrosome; structure; motion; p160ROCK; cytokinesis

*Abbreviations used in this paper: CD, cytochalasin D; DC, daughter centriole; GFP, green fluorescent protein; MC, mother centriole; nt, nucleotide; ROCK, Rho-associated coiled-coil–containing protein kinase; PCM, pericentriolar material.

The Journal of Cell Biology, Volume 157, Number 5, May 27, 2002 807–817
http://www.jcb.org/cgi/doi/10.1083/jcb.200203034

directed against isolated centrosomes. One of these antibodies, mAb 6C6, reacted with the centrosome or microtubule-organizing centers in a wide variety of animal and plant cells (Chevrier et al., 1992). Here, using this antibody we have identified the Rho-dependent protein kinase p160ROCK as a PCM component. p160ROCK is important for actin organization and coordinated microtubule regulations (Ishizaki et al., 1996, 1997; Matsui et al., 1996; Narumiya et al., 1997; Hirose et al., 1998; Amano et al., 2000; Kosako et al., 2000). We report that p160ROCK is also required for centriole positioning and is essential for MC movement toward the midpiece in late telophase, hence for signaling the end of cytokinesis.

Results

Centrosomal localization of p160 ROCK

In a screen of an MDBK cDNA expression library with mAb 6C6, one positive clone (clone N) coded for a 438 amino acid polypeptide showing 98% sequence homology with a peptide sequence belonging to the kinase, p160ROCK (Fig. 1 A). This data raised the possibility that p160ROCK was present on centrosomes. To test this possibility, protein N was expressed in bacteria and used to generate a polyclonal antibody (antibody N). Epitopes recognized by the antibody were then mapped using peptide array analysis (SPOT analysis) (Fig. 1 B). Nine peptide clusters reacted with the antibody N on SPOT membranes (peptides N1–N9). Five peptide-specific antibodies were further derived from the antibody N using affinity chromatography with peptides N2, N3, N5, N6, and N7, respectively (Fig. 1 C). On Western blots of total protein extracts from MDBK cells, these antibodies reacted with a single 160-kD band corresponding to p160ROCK (Fig. 2 A). The same antibodies reacted with a 160-kD band on immunoblots of centrosomal fractions and also reacted with an additional protein of slightly smaller apparent molecular weight (Fig. 2 A). This latter protein may be a proteolytic product of p160ROCK generated during centrosome preparation or a specific centrosomal variant of p160ROCK whose structure remains to be determined. The antibodies also brightly stained centrosomes in different cell lines including MDBK and HeLa cells. The staining was concentrated on the MC and on an apparent linker structure between the centrioles (Fig. 2 B). Similar centrosome staining was observed with other p160ROCK antibodies, including commercial antibodies, ROCK-1 (C-19) antibody, and an affinity purified antibody raised against peptide N6-stained centrosomes (unpublished data). Immuno EM examination of centrosomes isolated from human KE37 lymphoblastic cells also showed intense staining of the intercentriolar linker (Fig. 2 C). The difference in labeling between the mother and DC was not clear on immuno EM images may be due to some degree of PCM dispersion during centrosome purification and absence of signal summation in centrosome sections.

We used RNA interference to test directly whether the centrosomal staining observed with p160ROCK antibodies corresponded to p160ROCK. HeLa cells were transfected with four different silencing RNA (siRNA) oligoduplexes corresponding to different coding regions of the p160ROCK

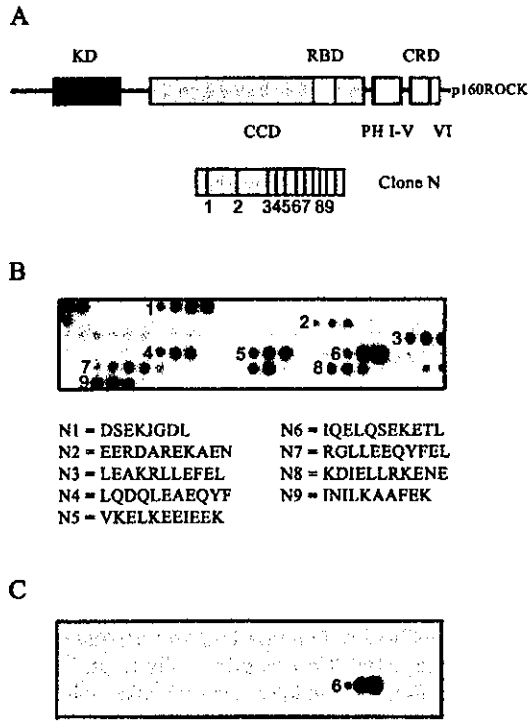

Figure 1. **Structure of clone N.** (A) Schematic representation of p160ROCK and clone N. p160ROCK (sequence data available from GenBank/EMBL/DDBJ under accession no. U43195) is a 160-kD protein serine/threonine kinase containing a kinase domain (KD), a long amphipathic α-helix capable of forming a coiled-coil structure (CCD) containing a Rho binding domain (RBD), the pleckstrin homology domain (PHI-V, VI) split by a cysteine-rich zinc finger (CRD); clone N (sequence data available from GenBank/EMBL/DDBJ under accession no. AY025529) coded for a protein fragment (protein N) corresponding to amino acids 594–1028. The positions of the nine epitopes recognized by polyclonal antibody directed against protein N (see B) are indicated. (B) Peptide SPOT analysis of the epitopes recognized by protein N polyclonal antibody showing nine positive peptide clusters (1–9). The sequences of the nine corresponding epitope peptides are shown below (N1 to N9). (C) Peptide SPOT analysis of the affinity purified N6 antibody. The affinity purified antibody reacted exclusively with peptide N6.

mRNA. Immunoblot analysis of total cell extracts showed p160ROCK depletion in cells exposed to siRNA (Fig. 2 D). In the presence of each one of the siRNA oligoduplexes, a substantial proportion of cells showed nuclear condensation and major disturbances of the microtubule cytoskeleton. These cells were not further analyzed. Among cells with apparently normal nuclei and microtubule content, cells with a conspicuously abnormal morphology, typical of p160ROCK inhibition (Hirose et al., 1998; Tominaga et al., 1998) were observed. Such cells have an irregular or elongated shape with characteristic cell extensions (Fig. 2 E; see Fig. 4, A and B). For each one of the four siRNA duplexes, a total of <100 cells showing abnormal morphology were examined for centrosome staining with p160ROCK antibody. This centrosome staining was uniformly absent. Cells transfected with mutated siRNA duplexes had normal morphology and always showed centrosome staining with p160ROCK antibody as nontransfected control cells (unpublished data).

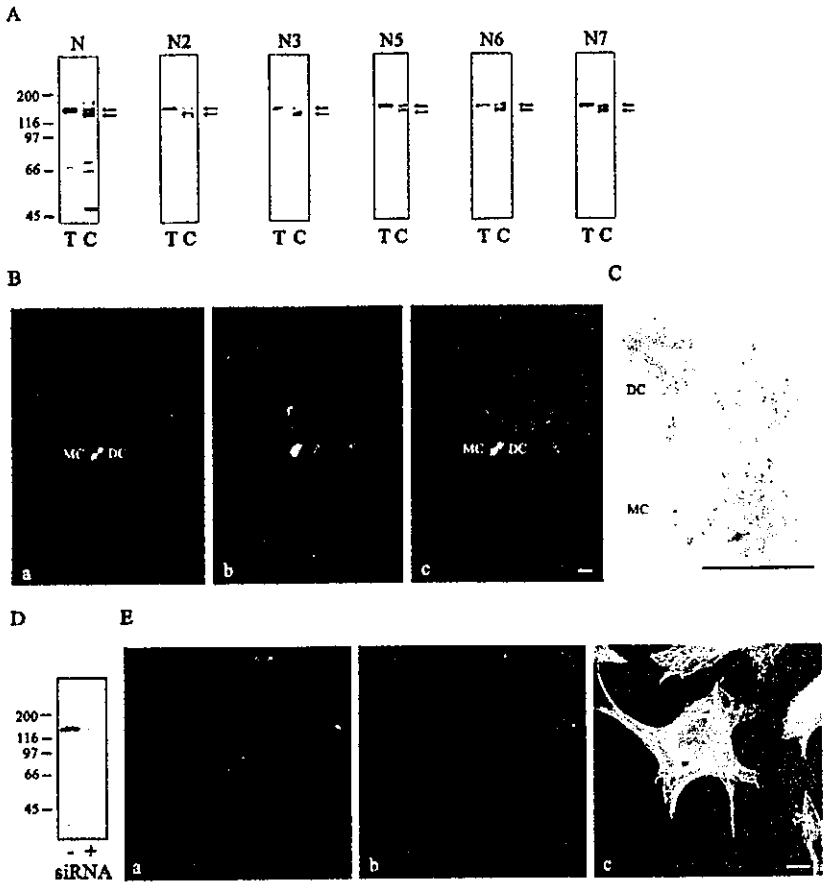

Figure 2. **Centrosomal localization of p160ROCK.** (A) Immunoblot analysis of total protein extracts from MDBK cells (T) and purified calf thymus centrosomes (C) using antibodies N, N2, N3, N5, N6, and N7. In total cell extracts, the peptide-purified antibodies reacted with a single 160-kD protein corresponding to p160ROCK. In centrosomal fractions, the same antibodies also stained a slightly lower molecular weight protein that may be a proteolytic product of p160ROCK or a centrosomal variant of this protein. (B) Immunostaining of HeLa GFP-centrin cells (a) with N6 antibody (b). The MC and DC were identified based on the centrin signal by conventional fluorescence microscopy examination of the cells. On visual examination, the MC shows distinctly stronger centrin signal than the DC (Piel et al., 2000). This difference is still visible although often less striking in confocal images. Bar, 1 μm. (C) Immuno EM localization of p160ROCK with polyclonal antibody N6 in isolated KE 37 centrosomes showing staining of the PCM, including the intercentriolar linker. Controls run with secondary antibody alone showed a complete absence of staining (unpublished data). Bar, 1 μm. (D) Silencing of p160ROCK: immunoblot analysis of p160ROCK in total cell extracts from either control HeLa cells or from HeLa cells transfected with siRNA n°3 (72 h after transfection), using p160ROCK antibody N6 as a primary antibody. Equal amounts of total cell protein from control and transfected cells were loaded as estimated from Coomassie blue gels (unpublished data). (E) Centrosome staining in HeLa GFP-centrin cells transfected with siRNA: cells were transfected with siRNA n°3. (a) Centriole visualization with GFP-centrin; (b) centriole staining with p160ROCK N6 antibody; (c) microtubule staining with anti-β-tubulin antibody. Changes in cell shape were used as a criteria for p160ROCK depletion. The figure is centered on a cell with abnormal shape, showing absence of centrosome staining with p160ROCK antibodies. The cell was surrounded by cells of normal shape, showing p160ROCK centrosome staining. Bar, 5 μm.

These results yield compelling evidence for a centrosomal localization of p160ROCK.

Effect of p160ROCK inhibition on centriole splitting

The centrosomal localization of p160ROCK raised the possibility that p160ROCK activity could affect centrosome structure or activity. We used several independent methods of p160ROCK inhibition to test this possibility.

We first examined the effect of the p160ROCK inhibitor Y-27632 (Uehata et al., 1997) in HeLa cells stably expressing green fluorescent protein (GFP) centrin stained with antibody N6 (Fig. 3). In control cells, centrosome staining was observed at all phases of the cell cycle. In late G2 cells, both centrosomes were stained, and the specific labeling of the linker structure evident in G1 was not visible (Fig. 3, d–f). Centriole staining with antibody N6 persisted through mitosis and cytokinesis. In the presence of Y-27632, the intercentriolar distance in G1 cells was generally conspicuously increased compared with controls (Fig. 3, a–c and a′–c′). When centrioles were split, the MC staining persisted, but no distinct staining of a linker structure was detectable (Fig. 3, a′–c′). Y-27632 had no apparent influence on centrosome staining in G2, metaphase, or anaphase cells. In telophase cells, treatment with Y-27632 induced a concentration of p160ROCK labeling in the cell midzone (Fig. 3, j′–o′).

The intercentriolar distance increased in cells treated with 10 μM Y-27632 (Fig. 4 A, f and h), but the drug effect was maximal with 100 μM Y-27632 (Fig. 4 A, j and l). Treated cells tended to elongate microtubules to form parallel bundles (Fig. 4 A, e and i), whereas actin stress fibers disappeared (Fig. 4 A, g and k). After drug withdrawal, microfilament and microtubule networks and the cell shape apparently went back to normal within 2–4 h (Fig. 4 A, m and o). In contrast, the intercentriolar distance remained elevated (Fig. 4 A, n and p).

When cells were transfected with the p160ROCK mutant KDIA, which acts as a dominant negative (Ishizaki et al., 1997), similar morphology changes and centrosome splitting (Fig. 4 B) were observed as in Y-27632–treated cells. Similar changes were also observed with siRNAs (Fig. 2 E).

In quantitative study of p160ROCK inhibition, the average intercentriolar distance increased threefold in the presence of 100 μM Y-27632 (Fig. 5 A) with a half-maxi-

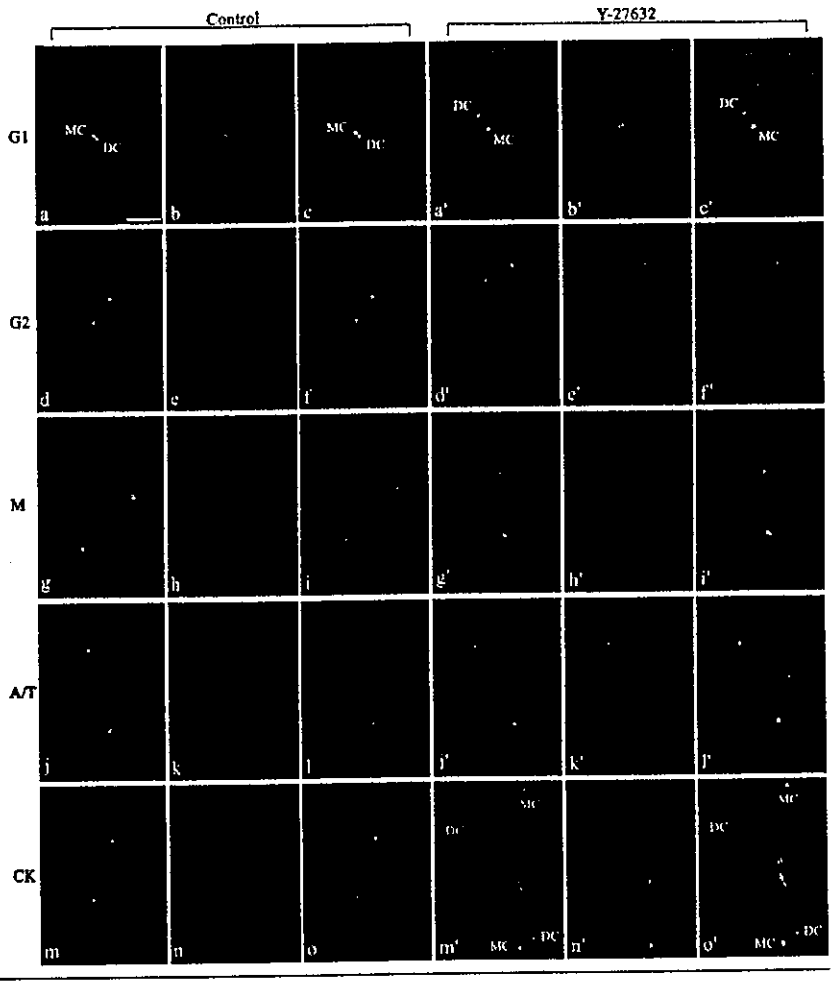

Figure 3. **Cell cycle changes in the distribution of p160ROCK.** Immunofluorescence of HeLa GFP-centrin cells with N6 antibody. Centrioles are visible as green dots (a, a', d, d', g, g', j, j', m, and m'). The red staining corresponds to N6 antibody staining (b, b', e, e', h, h', k, k', n, and n'). Merged images: c, c, f, f', i, i', l, l', o, and o'. Cells are shown in G1 phase (a–c and a'–c'), G2 phase (d–e and d'–e'), metaphase (M; g–i and g'–i'), late anaphase through early telophase (A/T; j–l and j'–l'), and cytokinesis (CK; m–o and m'–o') in the absence (a–o) or presence (a'–o') of the p160ROCK inhibitor Y-27632. The MC and DC were identified as in Fig. 2. Bar, 5 μm.

mal effect within 45 min after cell exposure to the drug. After drug withdrawal, no significant changes in the average intercentriolar distance were observed within 4 h (Fig. 5 B). Cell shape changes were quantified, using as an index the ratio of the cell perimeter to the cell surface (Fig. 5 C). When cells were treated for 1.5 h with 100 μM Y-27632, the perimeter to surface ratio increased significantly in the presence of the drug but went back to control values within 2 h after drug withdrawal, whereas centriole separation persisted (Fig. 5, B and C).

Increases of the perimeter to surface ratio and of the intercentriolar distance were also observed in cells transfected with the KDIA construct or with siRNA (Fig. 5, D and E). Thus, similar centrosome splitting was observed using three independent methods for p160ROCK inhibition.

Effect of p160ROCK inhibition on centrosome positioning

We used videomicroscopy to investigate the effect of p160ROCK inhibition on centriole positioning. Centrioles display little motion during the S and G2 phases of the cell cycle. In contrast, centrioles can show important motion in G1 when the DC transiently shows excursion through the cell cytoplasm in migrating cells, and in late telophase, when the MC leaves its central position and migrates toward the midbody (Piel et al., 2001). Cell exposure to 100 μM Y-27632 did not change centriole behavior in S or G2 cells (unpublished data). In late anaphase cells exposed to the drug, the MC movement toward the midbody remained of normal amplitude and duration (Fig. 6). In contrast, after abscission and exit from mitosis major changes affected the MC behavior, which instead of being almost immobile and positioned near to the cell center as in control cells displayed persistent motion (Fig. 6, A and B), often being located near the cell periphery. Although in control cells both centrioles remained in close vicinity, except for short periods of time (Fig. 6 A, 03:24 and 03:28, and B), in treated cells the two centrioles were often widely separated (Fig. 6, A and B). After drug withdrawal, the MC behavior was back to normal within 2 h, and the organelle slowly relocated to the cell center. However, the two centrioles usually failed to cluster, and the intercentriolar distance remained elevated (Fig. 6 B).

In G1 cells treated with Y-27632 after cytokinesis, the MC left its normal central position within a few minutes after addition of the drug, moving away from the DC and undergoing erratic motion. The MC frequently moved back and forth along the plasma membrane (Fig. 7 B). In some cases, it circled the nucleus (Fig. 7 B).

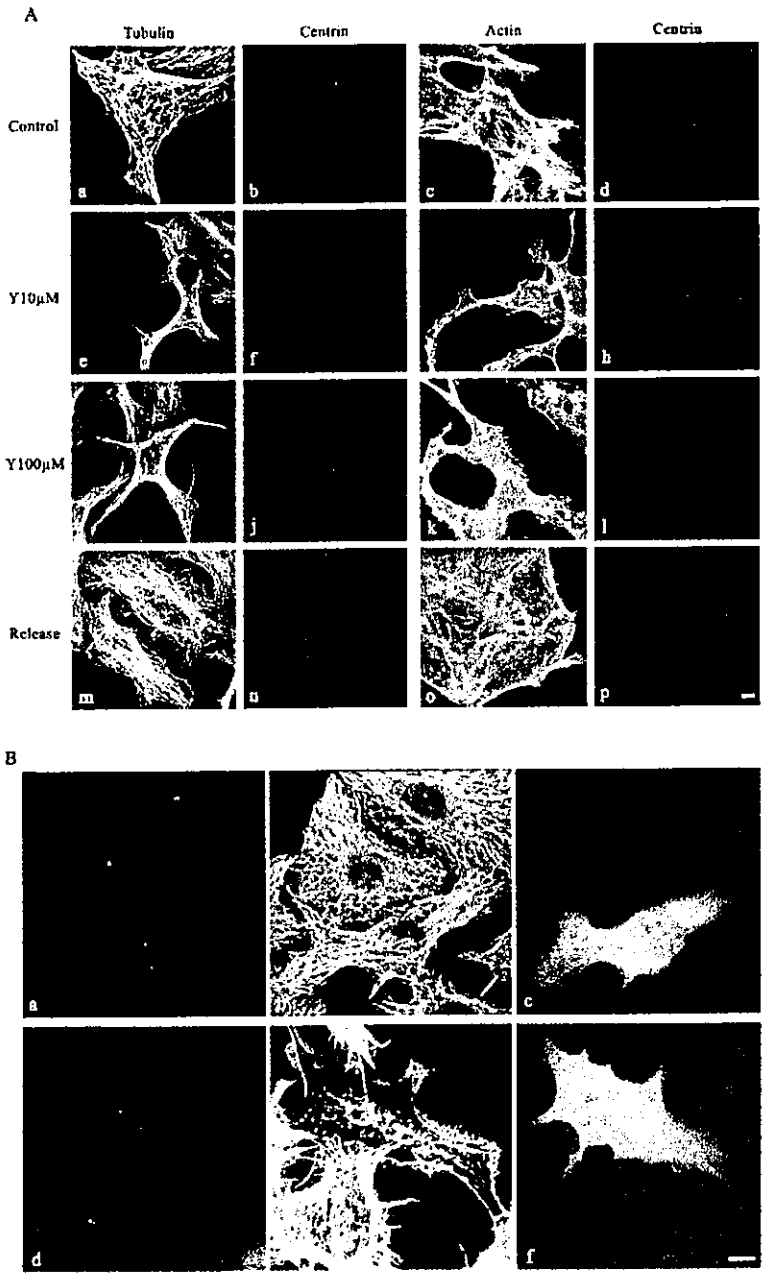

Figure 4. **Centrosome splitting by p160ROCK inhibition.** (A) Immunostaining of HeLa GFP-centrin cells with monoclonal anti-β-tubulin antibody or phalloidin-rhodamine. Untreated cells (a–d); cells treated for 1.5 h with 10 μM Y-27362 (e–h); cells treated with 100 μM Y-27362 for 1.5 h (i–l); cells treated with 100 μM Y-27362 for 1.5 h (m–p) examined 4 h after withdrawal of the drug. Exposure to the drug caused cell shape changes, stress fiber disruption, and centrosome splitting. Centrosome splitting persisted after drug withdrawal. Bar, 5 μm. (B) Immunostaining of HeLa GFP-centrin cells transfected with cMyc-tagged p160ROCK dominant negative KDIA construct. Cells were examined 24 h after transfection. GFP-centrin (a and d); tubulin staining (b); phalloidin-rhodamine staining (e); c-Myc staining (c and f). c-Myc–positive cells showed abnormal shape, stress fiber disruption, and centrosome splitting as Y-27632–treated cells. Bar, 5 μm.

In the presence of nocodazole, the effect of Y-27632 on the MC movement was inhibited (Fig. 8). In contrast, a 30-min treatment with cytochalasin D (CD) preceding Y-27632 addition did not modify the MC behavior. Thus, the MC movements induced by Y-27632 were microtubule dependent but actin independent as reported previously for the telophase MC movement (Piel et al., 2001). Cytochalasin treatment suppressed the DC motion (Fig. 8) as previously observed (Piel et al., 2000).

Centriole movements were also examined in cells transfected with KDIA mutant. In transfected G1 cells, MCs showed the same erratic motions around the cells as in cells treated with Y-27632 (unpublished data).

p160ROCK inhibition triggers MC migration toward the midpiece and subsequent completion of cytokinesis in postanaphase cells

After our observations of centriole separation and MC delocalization after p160ROCK inhibition, we wondered whether p160ROCK inhibition could trigger MC migration in the midbody in postanaphase cells. To test this possibility, postanaphase cells isolated by mitotic shake off were treated with Y-27632 1 h after replating, and the percentage of pairs of daughter cells with a centriole in the midbody region bridge was monitored over time (Fig. 9 A). The percentage of cells linked by a cytoplasmic bridge was determined at the same time points (Fig. 9 B). Centriole

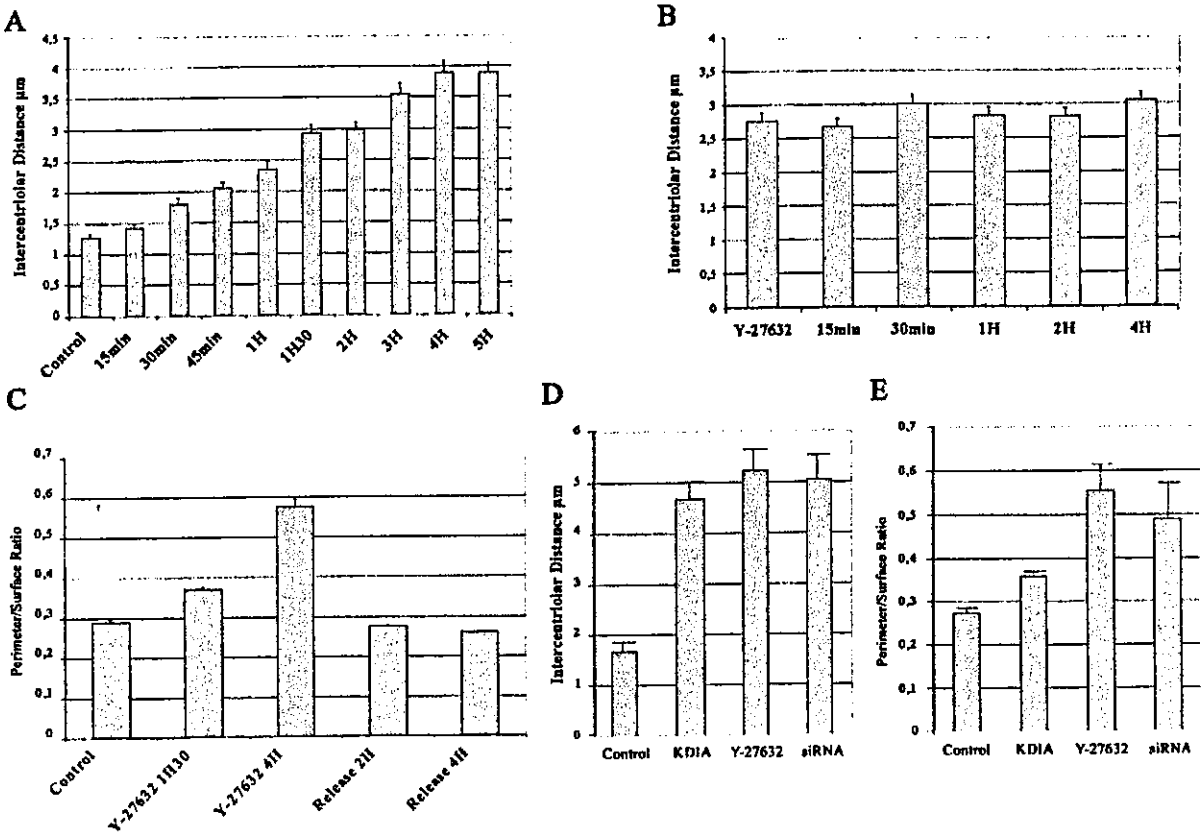

Figure 5. **Quantitative analysis of intercentriolar distance and cell shape after p160ROCK inhibition.** (A) Average intercentriolar distances in cells treated with 100 µM Y-27632 for the indicated amounts of time. In each condition, the average intercentriolar distance was measured on a minimum number of 200 cells. SEMs are indicated. (B) Average intercentriolar distances in cells treated with 100 µM Y-27632 for 1.5 h and then left to recover for the indicated amounts of time after drug withdrawal. Cell numbers and SEMs are as in A. (C) Perimeter to surface ratios in cells treated with 100 µM Y-27632. Cells were treated with Y-27632 for the indicated amounts of time and then fixed and processed for analysis. In release experiments, cells were treated with 100 µM Y-27632 for 90 min, then the drug was withdrawn, and at the indicated times after release from the drug, cells were fixed for subsequent analysis. In each condition, a minimum of 50 cells was examined. The perimeter to surface ratios showed little dispersion, and in some conditions SEMs were too small to be visible on the figure. (D) Average intercentriolar distances after p160ROCK inhibition with 100 µM Y-27632, KDIA mutant, or siRNA as indicated. Cells were treated with Y-27632 for 4 h before analysis. KDIA-transfected cells were analyzed 24 h after transfection. For siRNA-treated cells, the analysis (48 h after transfection) concerns cells with extinct p160ROCK signal, normal nuclei, and assembled microtubule arrays. In each condition, the average intercentriolar distance was measured on a minimum number of 100 cells. SEMs are indicated. (E) Perimeter to surface ratios after p160ROCK inhibition. Conditions were as in D.

migration in the midbody occurred prematurely in treated cells compared with controls with a frequency maximum at 30 min after exposure to the drug compared with 1.5–2 h in controls (Fig. 9 A). This maximum was up to 60% in drug-treated cell pairs compared with <15% in control cell pairs. Thus, there was a striking synchronization effect of drug treatment on MC localization in the midbody. Additionally, the proportion of cells linked by a cytoplasmic bridge dropped prematurely in drug-treated cells compared with control cells and then continued to diminish more rapidly over time (Fig. 9 B), indicating that the drug-induced MC migration to the midbody was followed by abscission.

Discussion

Centrosomal localization of p160ROCK

Our data show association of p160ROCK with the PCM surrounding the MC and with an intercentriolar linker structure in G1 cells. Apparently, the DC recruits p160ROCK during duplication. Several proteins show transient or permanent-specific association with the MC including ninein (Mogensen et al., 2000), cenexin, or ODF2 (Lange and Gull, 1995; Nakagawa et al., 2001) and epsilon tubulin (Chang and Stearns, 2000). Our data identify p160ROCK as an additional marker of the MC.

On EM images of isolated centrosomes, the MCs and DCs are bridged by a distinct linker structure (Bornens et al., 1987). However, markers of this structure in intact cells have been lacking, and this has lead to doubts concerning the existence of an intercentriolar linkage in vivo (Jean et al., 1999). Our data provide strong evidence for a localization of p160ROCK on the linker both in vitro and in vivo. Therefore, the enzyme emerges as a new marker of the linker in cells.

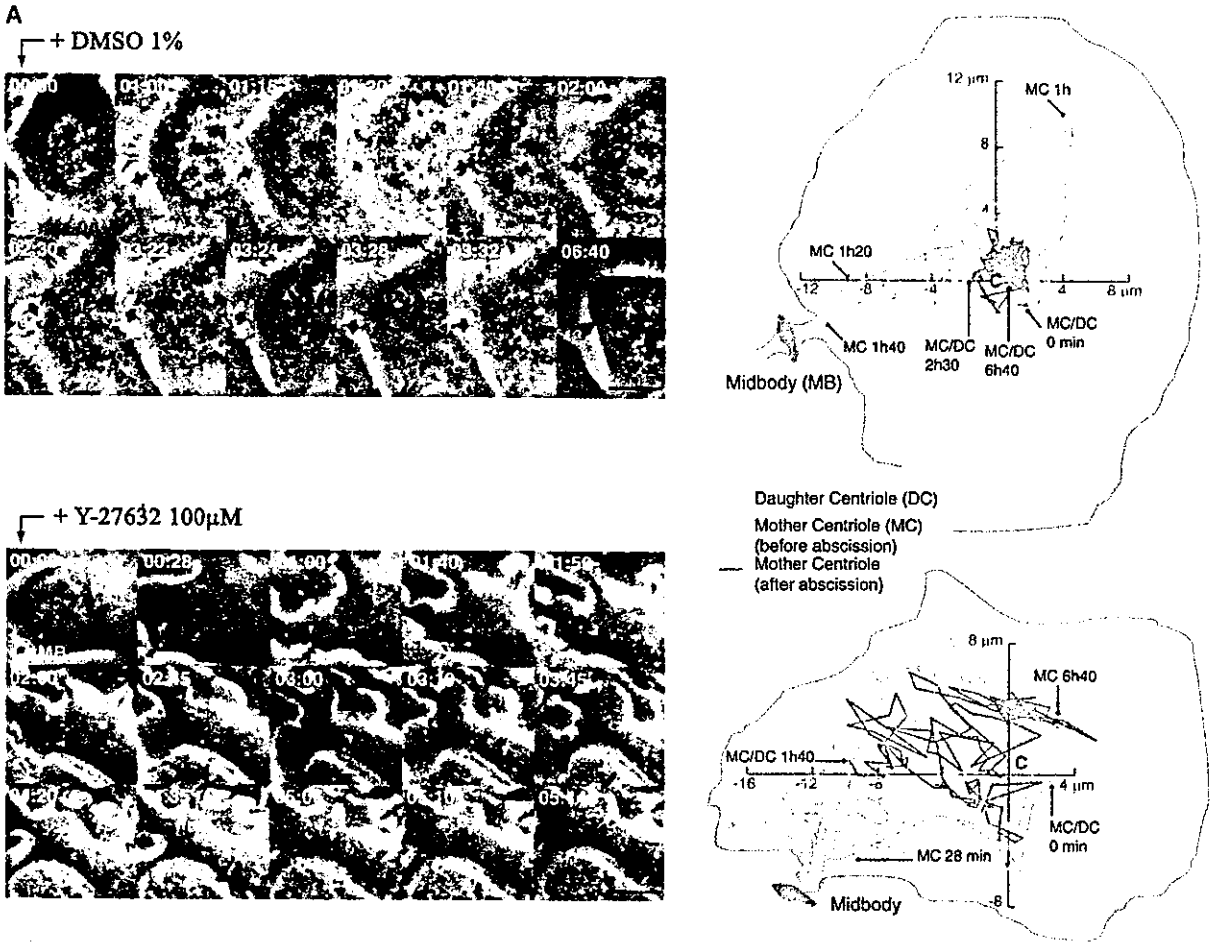

Figure 6 (continues on next page)

Effects of p160ROCK inhibition on centrosome structure and behavior

We find that p160ROCK inhibition triggers a permanent centriole splitting in G1, persisting for hours after release from inhibition when cells had recovered apparently normal cytoskeleton, shape, and centriole motion. This is a strong indication that p160ROCK inhibition causes changes in centrosome structure, namely in the intercentriolar linker, which seems to be an important determinant of the intercentriolar distance in G0-G1 cells (Komesli et al., 1989). The apparent irreversibility of the centrosome splitting and the disappearance of the p160ROCK staining of the intercentriolar area observed in G1 cell exposed to Y-27632 may correspond to a complete linker disruption. However, the loss of linker staining may be due to linker decondensation with resulting dilution of the signal. We have observed that even when centrioles are far apart in cells they seem to remain connected by a loose structure containing the matrix protein AKAP 450 and centrin (unpublished data).

We also find that p160ROCK inhibition induces wide MC excursions and relocation near the plasma membrane. This effect is actin independent but microtubule dependent and could involve a modification of microtubule dynamics through the action of cytoplasmic p160ROCK on microtubule dynamics or organization (unpublished data). Nevertheless, the centrosomal localization of a fraction or an isoform of p160ROCK suggests an action on the centrosome itself. p160ROCK inhibition has no evident effect on microtubule nucleation (unpublished data) but may affect microtubule anchoring or the anchoring of the MC in the surrounding cytoplasm.

The MC movements induced in G1 cells by p160ROCK inhibition share close similarity with the normal telophase movement of this centriole. Both movements involve wide excursions and relocation of the MC at the cell periphery and show similar differential sensitivity to nocodazole and CD. Additionally, previous work has shown down-regulation of Rho at the end of telophase (Kimura et al., 2000). We now show that p160ROCK inhibition in postanaphase cells is sufficient to trigger MC migration to the midpiece and subsequent abscission. Together, these data strongly indicate a central involvement of p160ROCK in triggering centrosome-dependent exit of mitosis in cycling cells.

In this study, Y-27632 and the p160ROCK dominant negative KDIA mutant had similar effects both inducing centrosome splitting and wide MC motility. This similarity in effects suggests a model in which centrosomal substrates

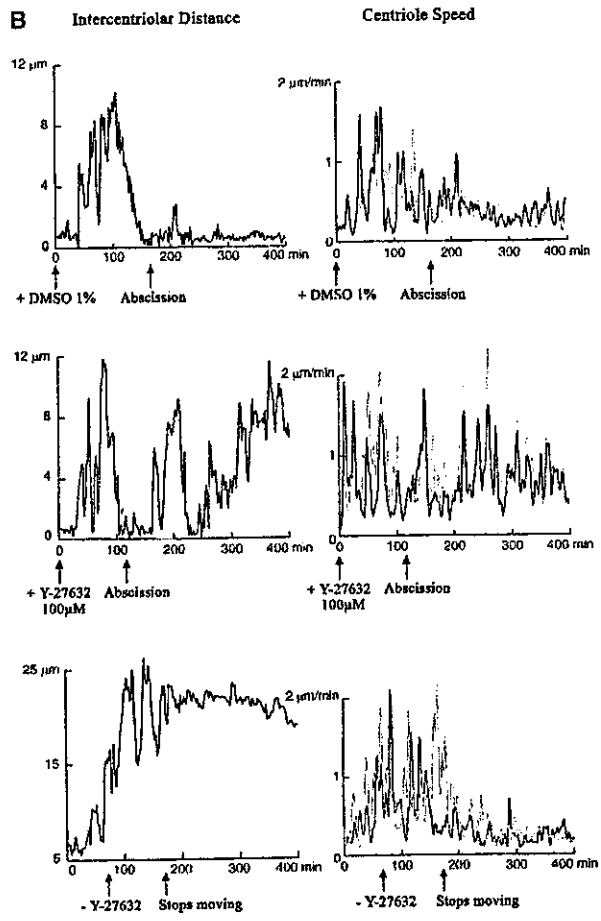

Figure 6. **Videomicroscopy analysis of Y-27632 effect on centriole motility.** Phase–contrast and fluorescence images of postmitotic and G1 Hela cells stably expressing GFP-centrin were recorded every 2 min. Cells were placed in a medium containing either DMSO (control cells) or Y-27632 as indicated. (A) The images on the left are extracted from movies. The corresponding time is indicated on the top left corner of each frame (h:min). An overlay of GFP signal (green) on the corresponding phase–contrast image is shown. The centrioles were spotted by hand with green dots to allow visualization at low magnification. The MC is the bigger one, indicated by a pink arrowhead before midbody rupture and a red arrowhead after midbody rupture. The DC is indicated by a gray arrowhead. Centriole trajectories are drawn on the right with the same color code. The cell margin at the beginning of the movie is indicated by a thin gray line. Thanks to the cytoplasmic fluorescence of the soluble GFP-centrin pool, the cell shape could be tracked automatically, and then the centroide of the cell was calculated for each plane. Centriole position is shown relatively to that centroide, which is thus the point 0 of the coordinates (indicated by C). Y-27632 was added at time 00:00. Bar, 10 µm. (B) The intercentriolar distance and the centriolar speed are plotted over time (gray curve, DC speed). The four top graphs correspond to the cells shown in A. The two bottom graphs correspond to a release experiment: Y-27632 was added 1 h before time 0, and then the cells were filmed during 1 h before the medium was replaced by Y-27632–free medium (three washings). In the case shown, the intercentriolar distance is elevated because the cell was elongated and the centrioles were on both sides of the cells when the drug was removed, resulting in an arrest of centriolar motion. The centrioles never clustered again after drug removal.

of p160ROCK are also binding partners of the enzyme. Y-27632 is known to inhibit p160ROCK catalytic activity by competing with ATP (Narumiya et al., 2000). In the presence of the drug, the unphosphorylated p160ROCK substrate partners may remain bound on the enzyme and never assemble into PCM structures. The same partners may be trapped by the cytoplasmic KDIA mutant and, in the presence of this mutant, never reach the centrosome.

SiRNA duplexes had additional deleterious effect on cells compared with Y-27632 or KDIA mutants, ultimately inducing cell death. This probably results from the complete elimination of all p160ROCK domains by RNA interference, whereas the two other methods leave extensive parts of the protein intact.

In conclusion, our data provide strong evidence that p160ROCK activity is important for both centrosome organization and positioning of the centrioles and that it plays a central role in centrosome-dependent cell exit of mitosis.

Materials and methods

Library screening and cDNA cloning and sequencing

A MDBK cDNA expression library (CLONTECH Laboratories, Inc.) was screened with a previously characterized monoclonal antibody mAb 6C6 (Chevrier et al., 1992) using standard procedures.

Expression and purification of recombinant proteins

The clone N cDNA was subcloned into pGEX-4T3 vector (Amersham Pharmacia Biotech). *Escherichia coli* BL21 cells were transformed with the pGex construct. Fusion protein induction and purification were done using standard methods.

Antibody production and purification

Immunization of rabbit was performed using 500 µg of purified N protein emulsified in complete Freund's adjuvant for the primary injection. Subsequent booster immunizations were performed on days 14, 28, 42, 56, and 70 using 500 µg of purified N protein emulsified in Freund's incomplete adjuvant. A test bleed demonstrated anticentrosome antibodies; preimmune serum was also collected and used for some control studies.

Serum was affinity purified against the purified N protein coupled to sepharose 4B. The bound antibodies were eluted using 10 vol of 0.1 M glycine, pH 2.5. The eluted antibodies were neutralized by the addition of 1 vol 1 M Tris HCl, pH 8.0, and the antibodies were dialysed against PBS and concentrated for long term storage.

For anti–N peptide antibodies, serum was affinity purified against each corresponding peptide coupled to sepharose 4B, and they were eluted as described previously.

SPOT analysis

SPOT synthesis corresponding to N protein was performed according to Frank (1992) with an Abimed ASP 222 automated SPOT robot. Peptide sheet was permeabilized in ethanol bath, washed three times (10 min each) with PBS 0.1% Tween 20 (PBST), and incubated 1 h at room temperature with purified polyclonal antibody anti–N protein (1:5,000) or anti-peptides N(1–9) (1:5,000) in PBST. After three washes (10 min each) in PBST, the membrane was incubated with anti–rabbit antibody labeled with HRP (1:5,000), washed three times as above, and developed using the chemiluminescent ECL kit (Amersham Pharmacia Biotech).

RNA interference

To design target-specific siRNA duplexes, we selected four sequences of the type AA(N19)dTdT from the ORFs of the p160ROCK mRNA (U43195) in order to obtain a 21-nucleotide (nt) sense and 21-nt antisense strand with symmetric 2-nt overhangs of identical sequence as described by Harborth et al. (2001). We used 2′ deoxythymidines instead of uridine residues in the 3′ overhangs to enhance nuclease resistance. The selected sequences were submitted to a BLAST search against the human genome sequence to ensure that only p160ROCK gene of the human genome was targeted. 21-nt RNAs were purchased from Dharmacon in deprotected and desalted form. The siRNA sequence targeting p160ROCK were from position relative to the start

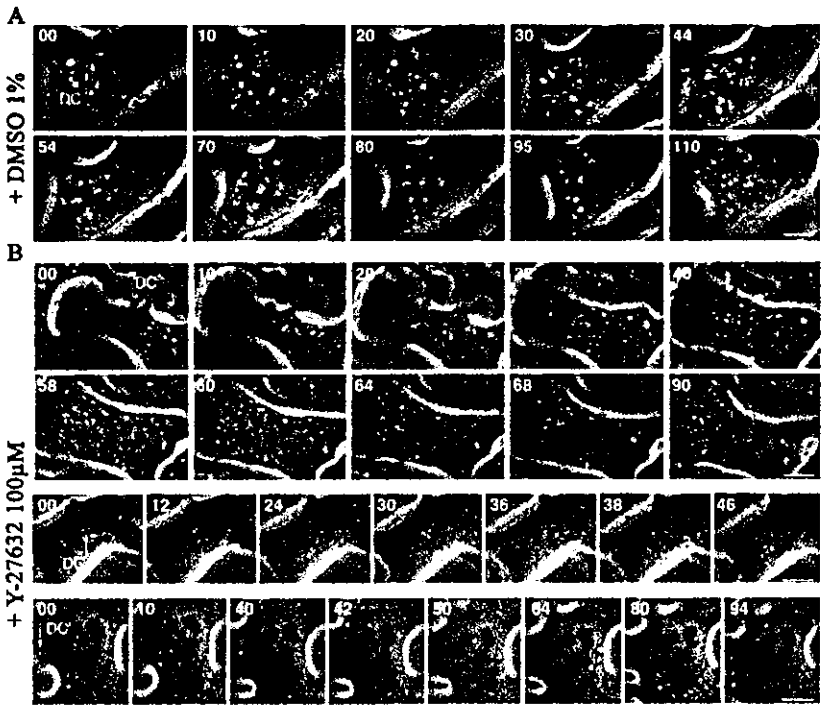

Figure 7. **Centriole behavior in G1 HeLa cells.** Centrioles are shown as in Fig. 6 A. G1 HeLa cells recorded as in Fig. 6. Time is in minutes. (A) Control cell; the MC stays near the cell center. (B) Three examples of characteristic behaviors of the MC in cells treated with 100 µM of Y-27632: either running along the membrane (first two rows) or turning around the nucleus (last row). Bar, 10 µm.

codon: n°1 = 566–584, n°2 = 639–657, n°3 = 1958–1976, and n°4 = 2780–2798. As unspecific siRNA control, we used siRNA n°3 mutated on three nucleotides. For annealing, 20 µM single-stranded 21-nt RNAs in annealing buffer (100 mM potassium acetate, 30 mM Hepes-KOH, pH 7.4, 2 mM magnesium acetate) for 1 min at 90°C followed by 1 h at 37°C.

Cell culture and transfection

MDBK cells were cultured in RPMI 1640 medium supplemented with 10% heat-inactivated bovine FCS, 2 mM glutamine, 1 mM sodium pyruvate, 100 IU/ml penicillin, and 100 µg/ml streptomycin at 37°C with 6.5% CO_2. HeLa cells stably expressing GFP-centrin were maintained using previously reported procedure (Piel et al., 2000).

To inhibit p160ROCK, cells were treated with 10 µM or 100 µM Y-27632 (provided by Yoshitomi Pharmaceutical Industries) for 15 min to 5 h at 37°C.

The day before transfection, cells were trypsinized, diluted with fresh medium, and transferred to 24-well plates (10^4 cells/well). For transient transfection of siRNA, Oligofectamine (Invitrogene) was used. 12 µl OPTIMEM medium (Invitrogen) and 3 µl Oligofectamine per well was preincubated for 10 min at room temperature. In parallel, 50 µl OPTIMEM medium was mixed with 3 µl siRNA (60 pmole). The two mixtures were combined and incubated for 20 min at room temperature. After addition of

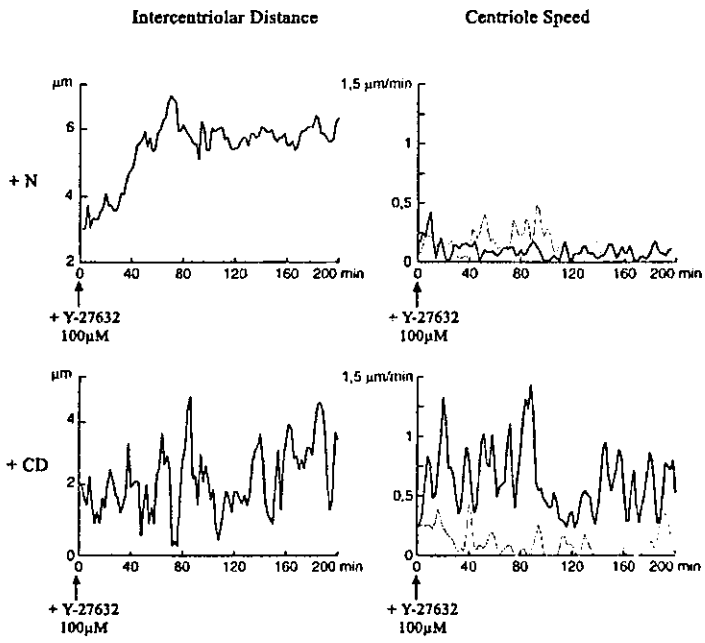

Figure 8. **Videomicroscopy analysis of nocodazole and cytochalasin effect on centrosomes in cells treated with Y-27632.** The intercentriolar distance and the centriolar speed are plotted over time (gray curve, DC speed). (Top graphs) G1 cells were treated with 5 µM nocodazole (N) and cold for 30 min to depolymerize microtubules and then rewarmed at 37°C and filmed in a medium containing nocodazole and 100 µM Y-27632. (Bottom graphs) Cells were treated with 1 mg/ml CD for 20 min and then filmed in the presence of CD and Y-27632.

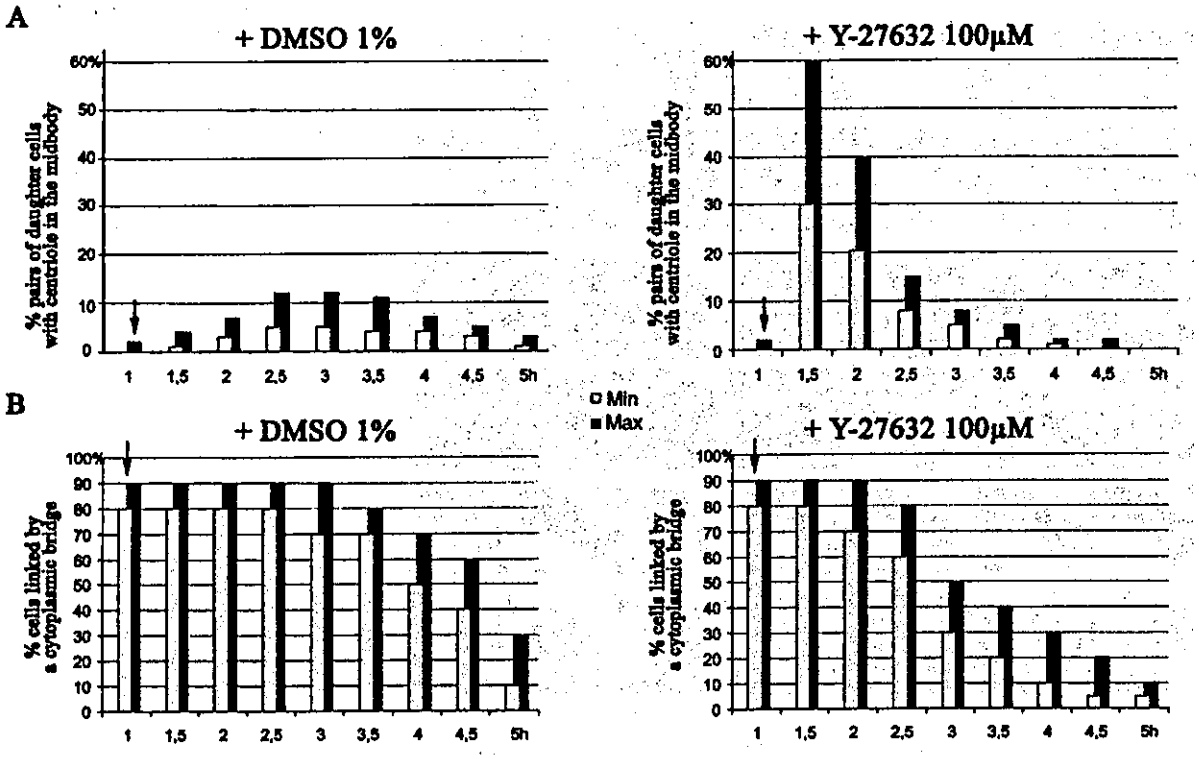

Figure 9. **Synchronization effect of p160 ROCK inhibition on MC movements and abscission.** Cells were treated either with 1% DMSO or 100 µM Y-27632 1 h after replating from a mitotic shake off (arrows). Coverslips were then fixed at indicated time points, and the percentages of both daughter cell pairs with centriole in the midbody (A) and cells linked by a cytoplasmic bridge (B) were determined. At least 300 cells were counted for each percentage determination. Four independent experiments were done. The maximum (max) and the minimum (min) values observed are indicated. Percentages do not add up to 100% because centriole localization in the midbody can escape detection and because of the statistical error attached to each percentage determination.

32 µl of OPTIMEM medium, the mixture was added to cells. Cells were usually assayed 48–72 h after transfection. For transient transfection with KDIA, a cMyc-tagged dominant negative mutant of p160ROCK (Ishizaki et al., 1997), Lipofectamine Plus reagent (Invitrogen) was used. Cells were transfected with 0.5 µg of DNA by the application of Lipofectamine DNA coprecipitates in DME (GIBCO BRL). The medium was changed to serum-free DME at 3 h, and then the cells were cultured for another 12 or 36 h.

Cell synchronization

Mitotic HeLa cells were pooled by mitotic shake off as described in Piel et al. (2001). They were then replated on fibronectin- and collagen-coated glass coverslips. After 45 min, unattached cells were gently flushed in order to minimize desynchronization due to the variation of reattachment time of mitotic cells.

Cell fractionation

MDBK cells or siRNA-transfected HeLa cells were grown on plastic dishes for 72 h. Whole cell extract were obtained by direct resuspension of cells in boiling 1% SDS. After sonication, cells extracts were centrifugated 20 min at 100,000 *g*. The supernatants were further denatured in Laemmli sample buffer (25 mM Tris, 1% SDS, 10% glycerol, 1% 2-mercaptoethanol) and boiling.

Centrosome preparation

Centrosomes were purified from calf thymocytes as in Komesli et al. (1989). Centrosomes were isolated from KE 37 cells as described by Bornens et al. (1987).

Immunofluorescence microscopy

In all immunofluorescence experiments, antibodies were diluted in PBS supplemented with BSA at 1 mg/ml. Dilution factors are indicated in parentheses.

HeLa cell stably expressing GFP-centrin were grown on coverslips and washed in PBS before further processing. Cells were generally fixed for 4 min in methanol at −20°C, but for actin staining cells were fixed for 10 min in 3.7% paraformaldehyde and permeabilized 10 min with PBS containing 0.5% Triton X-100.

The preparations were subsequently washed in PBS, incubated with primary antibody mouse monoclonal anti–β-tubulin antibody clone 2-1 (1:100; Sigma-Aldrich), monoclonal anti-myc antibody (1:100; Invitrogen), rabbit polyclonal anti–protein N (1:500), or rabbit anti–peptide N1 to N9 (1:100) followed by the appropriate secondary antibody goat anti–mouse conjugated with fluorescein (1:250; Jackson ImmunoResearch Laboratories), goat anti–rabbit conjugated with rhodamine (1:250; Jackson ImmunoResearch Laboratories), rhodamine phalloidine (1:50; Molecular Probes), or goat anti–mouse conjugated with Alexa fluor 350 (1:500; Molecular Probes). Preparations were examined in Leica TCS-SP2 laser-scanning confocal microscope. Measures of intercentriolar distance and of cell perimeter to surface ratios were performed using IPLab software (Princeton Instruments).

Immuno EM

KE 37–isolated centrosomes were sedimented onto coverslips and processed as described in Chevrier et al. (1995) with the exception that tannic acid treatment of the fixed samples was omitted.

Immunoblot analysis

Gel electrophoresis analysis of each protein fraction was performed in one dimension according to Laemmli (1970). Proteins were transferred onto PVDF Immobilon membranes according to Towbin et al. (1979). The membrane was saturated in PBS 0.1% Tween 20 at room temperature for 1 h, and all subsequent washes and antibody dilutions were performed in this buffer. The membrane was incubated for 1 h with either rabbit polyclonal N antibody (1:5,000) or anti-peptide N(1–9) antibodies (1:500). After three 10-min washes, the membrane was incubated for 1 h with HRP goat anti–rabbit